

CERTIFICATION OF APPROVAL

RESPONSES OF TENSION LEG PLATFORM (TLP) DUE TO WAVE AND CURRENT

by

Mohd Zhafran Bin Sulaiman

A project dissertation submitted to the
Civil Engineering Programme
Universiti Teknologi PETRONAS
in partial fulfillment of the requirement for the
BACHELOR OF ENGINEERING (Hons)
(CIVIL ENGINEERING)

Approved by,



(Assoc Prof. Dr Kurian V. John)

UNIVERSITI TEKNOLOGI PETRONAS

TRONOH, PERAK

January 2009

CERTIFICATION OF ORIGINALITY

This is to certify that I am responsible for the work submitted in this project, that the original work is my own except as specified in the references and acknowledgements, and that the original work contained herein have not been undertaken or done by unspecified sources or persons.



(Mohd Zhafran Bin Sulaiman)

ABSTRACT

As the oil and gas resources had been depleted, most of the oil and gas companies had focused in deep water exploration. To design a platform in deepwater, wave loading and environment loading such as wind and current need to be considered. This paper discuss about the responses of Tension Leg Platform (TLP) due to wave and current. The idea of this project is to find the motion and forces to the TLP with regards or influence of the current at certain locations. The case study is made with Ram Powell TLP in difference current velocities. The theories that were used in finding the motions and forces were 'Linear Airy Wave Theory', 'Pierson-Moskowitz Spectrum' and 'Motion Response Spectrum'. This project also conducts a literature survey about the type of TLP which are conventional TLP, SeaStar TLP and Moses TLP, The latest information of existing TLP, Numerical Analysis and Experimental Analysis of dynamic motion (surge, heave and pitch). The project will come up with tabulated result and some graphs about the responses of current on the TLP. From the results, there were clearly stated the percentage increment of responses due to various wave and current. Some discussion recommendations were included for continuation study and research on this topic.

ACKNOWLEDGEMENTS

Author wishes to take the opportunity to express his utmost gratitude to the individual that have taken the time and effort to assist the author in completing this project. Without the cooperation of these individuals, no doubt the author would have faced some complications throughout the project.

First and foremost the author's utmost gratitude goes to the author's supervisor, Associate Professor Dr Kurian V. John. Without his guidance, comments, valuable suggestion and kind patience, the author would not be succeeded to complete the project.

Appreciation and thanks are also extended to UTP Offshore Laboratory technician, Mr. Meor who had assist author in running experiment in the offshore laboratory.

A token of appreciation to the author's senior Mr. Rashdan, Mr. Azimi and Miss Azimah from the previous batch for their support and knowledge sharing. The author also would like to extend her appreciation to all his colleagues especially Mr. Ariff, Mr. Redzuan and Mr. Melvin Lau for their fully supports and collaboration. Last but not the least, the author wishes to express his heartfelt appreciation to his parents Mr. Sulaiman and Madam Wan Norashiha and family members for their moral support.

Hopefully, this work can be used and appreciated for those who are interested to make further studies or studies related to this field. The author felt very grateful to give contribution for the future development.

TABLE OF CONTENTS

CERTIFICATION OF APPROVAL	i
ABSTRACT	iii
ACKNOWLEDGEMENT	iv
TABLE OF CONTENTS	v
LIST OF TABLES	viii
LIST OF FIGURES..	ix
CHAPTER 1:	INTRODUCTION	1
	1.1 Background of Study	1
	1.2 Problem Statement	2
	1.3 Objectives and Scope of Study	3
CHAPTER 2:	LITERATURE REVIEW AND THEORY.	5
	2.1 Type of Platform.	5
	2.2 Tension Leg Platform (TLP).	5
	2.2.1 Conventional/Classic TLP.	7
	2.2.2 Extended TLP.	7
	2.2.3 Seastar TLP	8
	2.2.4 Moses TLP	9
	2.2.5 Tension Leg Platform (TLP) Component.	10
	2.3 Current Loads	12
	2.4 Linear Airy Wave Theory	12
	2.5 Morison Equation	13
	2.6 Pierson-Moskowitz spectrum.	14
	2.7 Wave Profile	14
	2.8 Motion-Response Spectrum	15

CHAPTER 3:	METHODOLOGY	16
3.1	Literature Survey.	16
3.2	Model selection of TLP	16
3.3	Numerical Analysis	16
3.3.1	Wave Spectrum	18
3.3.2	Surge calculation	18
3.3.3	Heave Calculation	20
3.3.4	Pitch Calculation	21
3.3.5	Response-Amplitude Operator (RAO) calculation	23
3.3.6	Responses (Surge, Heave, Pitch) Spectrum	23
3.3.7	Calculation for Different Current.	24
3.3.8	Results and Discussion	24
3.4	Experimental Analysis	25
3.4.1	Model scale down.	25
3.4.2	Model Fabrication	26
3.4.3	Laboratory Model Testing	26
3.5	Health safety and environment aspect.	30
3.6	Project schedule	30
3.7	Flow chart of the methodology	31
CHAPTER 4:	RESULTS AND DISCUSSION	32
4.1	Numerical Analysis	32
4.1.1	Pierson Moskowitz Spectrum	32
4.1.2	Surge Responses	34
4.1.3	Heave Responses	37
4.1.4	Pitch Responses	39
4.2	Experimental Analysis	42

CHAPTER 5:	CONCLUSION AND RECOMMENDATION.	47
5.1	Conclusion	47
5.2	Recommendation	49
REFERENCES		50
APPENDICES		51
Appendix A	Calculation for Natural period of Ribs	27
Appendix B	Resonance and Ultimate Harmonic Spectrum	27
Appendix C	Mean and Peak Spectrum for Current 0.00sec, 0.20sec and 1.00sec	29
Appendix D	Secondary Transverse Analysis	41
Appendix E	Percentage correction to Experimental surge Response	46

LIST OF TABLES

Table 2.1	TLP all over the world	6
Table 4.1	Details of Ram Powell TLP	32
Table 4.2	Pierson Moskowitz spectrum and wave height for each frequency	32
Table 4.3	Total added mass and Natural period of surge motion	34
Table 4.4	Total force and surge motion spectrum	35
Table 4.5	Calculation for Natural period of Heave	37
Table 4.6	Pressure and Heave Motion Spectrum	37
Table 4.7	Moment and Pitch Spectrum for Current 0.00m/s, 0.50m/s and 1.00m/s	39
Table 4.8	Summary from numerical Analysis	41
Table 4.9	Percentage increment or Experimental surge Responses	46

LIST OF FIGURES

Figure 2.1	Conventional TLP	7
Figure 2.2	Extended TLP (a) Kizomba A ETLP (b) Magnolia ETLP	8
Figure 2.3	Seastar Tension Leg platform	9
Figure 2.4	MOSES type of TLP	9
Figure 2.5	Component of Tension Leg Platform	11
Figure 3.1	Added Mass For Surge	19
Figure 3.2	Surge Force Acting to the TLP	20
Figure 3.3	TLP subjected to vertical force	21
Figure 3.4	Total Moment Reaction to TLP	22
Figure 3.5	Model testing dimension	25
Figure 3.6	Fabricated model testing	26
Figure 3.7	Model set up in the wave flume	27
Figure 3.8	Position of the model in the wave flume	27
Figure 3.9	Model testing movement during the experiment	28
Figure 3.10	Calculating the laboratory model responses	29
Figure 3.11	Flowchart of project Methodology	26
Figure 4.1	Graph Pierson Moskowitz Spectrums	33
Figure 4.2	Wave Elevation	34
Figure 4.3	Graph of Surge Spectrum	36
Figure 4.4	Graph of Surge Responses	36
Figure 4.5	Graph of Heave motion Spectrum	38
Figure 4.6	Graph of Heave motion Responses	38
Figure 4.7	Graph of pitch motion spectrum	40
Figure 4.8	Graph of pitch responses	41
Figure 4.9	Surge responses for wave with no current	42
Figure 4.10	Graph of Experimental surge responses for wave frequency 0.25Hz	43
Figure 4.11	Graph of experimental surge responses for wave frequency 0.35Hz	44
Figure 4.12	Graph of experimental surge responses of wave frequency 0.45Hz	45

CHAPTER 1

INTRODUCTION

1.1 Background of Study

Recently the classes of offshore structure the Tension Leg Platform (TLP) is particularly well suited for deep water operation. Different with fixed structure such as jacket platform TLP cost does not radically increase with water depth. The TLP is vertically moored at each corner of the hull minimizing the heave, pitch and roll of the platform. This small vertical motion results is less expensive production equipment than would be required on TLP, (Chakrabarti, 1987)

The surge, sway and yaw resonance frequencies of TLP's are below that of the wave frequency range as defined by a power spectrum such as the Pierson-Moskowitz. The heave, pitch and roll resonance frequencies are above this range. The resulting response is a desirable feature of TLP's. Wind, waves and current will cause a TLP to oscillate about an offset position rather than its vertical position. This offset in the surge direction has a corresponding set down, the lowering of the TLP in the heave direction, which increases the buoyancy forces. This result in a higher tension in the tendon than if it was in the vertical position. Higher-order effects due to the nonlinear nature of the waves and nonlinear structural properties will affect the dynamic response and may be of interest.

In designing the TLP, only the maximum value of current at the specific place had been taken into the consideration in designing TLP. Certain value of current and wave will give responses varies with other value of current and wave. These

responses need be studies to give more clear view of the responses of TLP due wave and current.

Model can be categorized in two major categories which are display model and engineering model. Engineering model is used to collect useful data in the design of structure. From the modeling testing, the behaviors of the original structure can be determined. (Chakrabarti, 1994)

1.2 Problem Statement

In a present time, oil and gas industries vigorous increase not only at Gulf of Mexico and North Sea but also in others region. A continues development of new technology for exploration, production are required to explore the potential petroleum field. In the early phase of oil and gas exploration, the water depth had been a major challenge in offshore structure design and economical value.

Nowadays the oil resources at shallow water had depleted. As a solution exploration to the deep water and ultra deep water had been started by most of the oil and gas companies. As water depth increases, the cost of jacket platform increases exponentially. To minimize the cost for deepwater offshore platform, TLP is one of the alternatives that can be used. TLP have widely been operating for the exploration and production of ocean resources, and many TLP now in operation.

The TLPs are required to be properly designed in order to keep it in position at certain water depth when they are subjected to external forces induced by ocean current, wind and waves. The Effect of current and wave of TLP need to be determine to make sure it comply the requirement and safe to be use.

Even though the TLP had been constructed and operated, it may cause some failure such as tendon breaking. The maintenance and repair need to be done in the same time to keep the TLP in allowable distance of responses. With respect to various value wave and current that subjected to TLP, the responses need to be analyzed to make sure during the maintenances the displacement will not exceed the tolerance.

1.3 Objective and Scope of Studies

1.3.1 The objectives of this research are;

- To prepare a detailed literature survey report about the tension leg platforms (TLP) existing and under design /construction stage.
- To analyze the motion and tether forces of the platform subjected to random wave and current.
- To determine the effect of various current speed on the responses.
- To test a model in the wave tank or wave flume and determine the responses for comparison with analytical projects.

1.3.2 The scopes of this research are;

The detailed literature will be limited from Information Resources Centre Universiti Teknologi PETRONAS (IRCUTP). The analysis of the motion will only consider the frequency domain dynamic analysis. The environmental loading will consider the Pierson-Moskowitz (PM) Spectrum and the current velocity of 0.50m/s and 1.00m/s. For the model testing, the dimensions will be fixed based on the budget that had been allocated by the university

1.3.3 The relevancy of the project

There relevancy of the project are, for Malaysia Oil and Gas company (PETRONAS) will not designing the Tension leg Platform (TLP) or other type of offshore platform. During the operation of the offshore platform if there is a maintenance problem such as damage or breaking tendons, Oil and Gas company or the operator company can do it by their own expertise and have not need to find any outsourcing company to solve the problem. They can do by their own. This can really save a lot of their money.

During the maintenance and repair process the responses of wave and varies current need to be analyzed to keep the TLP or other offshore platform in condition with allowable displacement.

- Fixed platform (Shallow water)
 - a. Jacket Platform
 - b. Gravity Base Structure (GBS)
- Crude oil Platform (Deep water)
 - a. Articulate Tower
 - b. Caisson Tower
 - c. Tension Leg Platform (TLP)
- Floating (Deep water)
 - a. Spar Platform
 - b. Semi-submersible

2.1 Tension Leg Platform (TLP)

Tension Leg Platform (TLP) is a buoyant platform held in the place by a tension system. That's are similar to the jacket platform and the difference is it maintain its position and the moorings held in tension by the buoyancy of the hull. The tension

CHAPTER 2

LITERATURE REVIEW AND THEORY

2.1 Type of Platform

Offshore exploration was started in the nineteenth century. Two places where the oil and gas industries start in North Sea area and the Gulf of Mexico. Offshore structure is the structure that has no access to dry land and which is required to stay in position in all weathers position. In oil and gas industries there are three types of offshore platform which are;

- Fixed platform (Shallow water)
 - a. Jacket Platform
 - b. Gravity Base Structure (GBS)
- Compliant Platform (Deep water)
 - a. Articulate Tower
 - b. Guyed Tower
 - c. Tension Leg Platform (TLP)
- Floating (Deep water)
 - a. Spar Platform
 - b. Semi-submersible

2.2 Tension Leg Platform (TLP)

Tension leg Platform (TLP) is a buoyant platform held in the place by a mooring system. TLP's are similar to the jacket platform and the difference is it maintain on position use the moorings held in tension by the buoyancy of the hull. The mooring

system is a set of tension leg or tether attached to the platform and connected to the templates or foundation on the sea floor.

The TLP concept was devised by the Conoco Oil Company as an alternative to fixed steel Structure and Floating production system (FPS) for the development of deep water oil and gas field. The first TLP was built in 1984 and used to develop the Hutton field in the North Sea. The water depth at Hutton TLP is 148m where it is the shallowest TLP. The deepest TLP is Conoco Magnolia TLP there the water depth is 11.4km. Magnolia TLP is located at Gulf of Mexico. Please refer to Table 2.1 for all the TLP around the world.

Table 2.1: List of TLP.

Tension Leg platform	Year	Type of TLP	Water Depth (m)
Hutton	1984	Conventional	147
Oveng	2007	New Generation-MOSES	271
Snorre	1992	Conventional	335
Heidrun	1995	Conventional	351
El-Paso Prince	2001	New Generation-MOSES	457
Okume/Ebano	2007	New Generation-MOSES	503
ENI Morpeth	1998	New Generation-SeaStar	518
Conoco Jolliet	1989	Conventional	536
Chevron/Texaco Typhoon	2001	New Generation-SeaStar	639
Matterhorn	2003	New Generation-SeaStar	859
Auger	1994	Conventional	873
Mars	1996	Conventional	896
Brutus	2001	Conventional	910
Ram-Powell	1997	Conventional	980
Marlin	1999	Conventional	988
Unocal West Seno 1	2003	Conventional	1021
Allegheny	1999	New Generation-SeaStar	1000
Ursa	1999	Conventional	1200
Kizomba A	2004	Conventional	1177
Kizomba B	2005	Conventional	1177
Neptune	2007	New Generation-SeaStar	1290
Marco Polo	2003	New Generation-MOSES	1311
Shenzi	2009	New Generation-MOSES	1311
Magnolia	2003	Conventional-Extension TLP	1432

In the world there are two types of Tension Leg Platform (TLP) which are Conventional TLP and New Generation TLP. New Generation TLP is divided into two types of TLP which are MOSES TLP and SeaStar TLP.

2.2.1 Conventional/Classic TLP

Conventional TLP normally there have four columns (Ram Powell TLP and Mars TLP) or six columns (Hutton TLP). There are four pontoons that are connected between the columns. Tendons are attached at the end of the columns and tight to the template. (Figure 2.1)

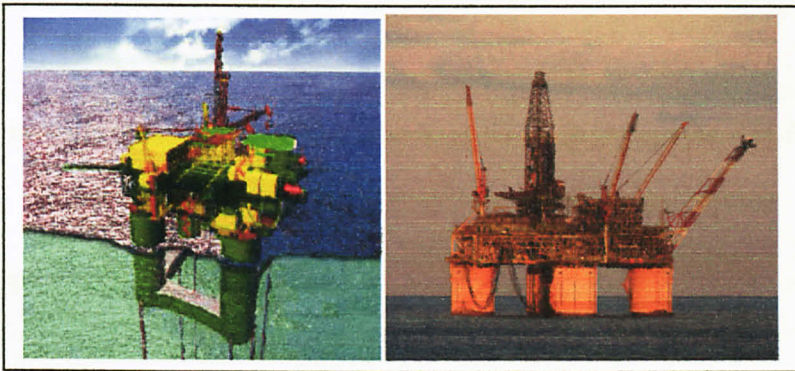


Figure 2.1: Conventional TLP

2.2.2 Extended TLP (ETLP)

The Extended Tension Leg Platform (ETLP) consists of four columns connected underwater by four pontoons. The pontoon extensions move the tendon connection point outboard of the columns. At the base of each column, a pontoon extends outward to support tethers, which are connected to pile foundations on the seabed.

The extensions effectively increase the restoring effect of the tendons while reducing the column spacing. This reduces the deck span between columns and thereby captures a saving in deck steel weight. The columns are circular for structural

efficiency and to minimize Environmental loading. The examples of ETLP are Magnolia ETLP, Kizomba A ETLP and Kizomba B ETLP. (Figure 2.2)

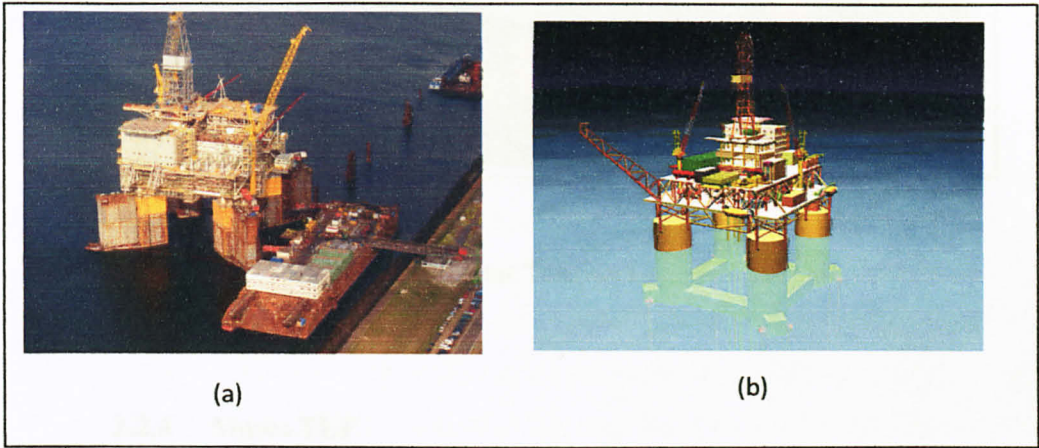


Figure 2.2: Extended TLP (a) Kizomba A ETLP (b) Magnolia ETLP

2.2.3 SeaStar TLP

SeaStar is a mini TLP that combines the simplicity of a spar and favorable response futures of a TLP. The SeaStar platform has application as an independent production platform on field having smaller reserves or as utility, satellite or early production platform for larger deepwater discoveries.

The Seastar TLP family had been developing to unlock the economic potential of discovered, but as yet undeveloped, deepwater field in the Gulf of Mexico and around the world. There are many Seastar TLPs operated in all over the world such as Chevron/Texaco Typhoon, Total Fina Elf Matterhorn, ENI Allegheny and ENI Morpeth. (Figure 2.3)



Figure 2.3: Seastar Tension Leg platform

2.2.4 Moses TLP

Moses TLP is different with conventional TLP because the column is rectangular shape and not circular shape. (Figure 2.4) The philosophy use in designing the Moses hull is to radially orient the four rectangular columns for improved water plane stability and improved deck structural support, thereby reducing deck spans and cantilevers, which reduced the size of the deck girders. Besides that, it has four outrigger tendon support structures (TSSs) to increase the tendon support footprint, thereby reducing the tendon loads. Example of Moses TLP is Oveng TLP, Prince TLP and Marco Polo TLP).



Figure 2.4: Moses type of TLP

2.2.5 Tension Leg Platform (TLP) Component

For conventional TLP the component for TLP consist of Topside, column, pontoon, Tendons or also called as tethers, riser (drilling production pipeline) and foundation templates (Figure 2.5)

A supporting structure of a TLP consists of hull, tendons and templates. The hull is a buoyant structure with a deck at its topside that supports the oil production facilities and crew accommodation. Pontoons and columns provide sufficient buoyancy to maintain the deck above the wave during all sea states. These columns are moored to the sea floor through tendons or tension leg, and fixed in the place with templates. The hulls buoyancy creates tension in the tendons.

Tension legs or tendons are tubular that secure the hull to the foundation. This is the mooring system for the TLP. Usually tendons are made from steel tubes with dimensions of 0.6-0.9 m (2-3 ft) in diameter with up to 3 inches of wall thickness, the length depending on the water depth. A typical TLP would be installed with as many as 16 tendons.

A template provides a frame on the sea floor in which to insert either conductors or piles. A foundation template may be one single piece or separates pieces for each corner. Then the foundation piles are driven through the foundation templates. The tether will be tight to the foundation templates to position the hull. Riser is the section of subsea pipeline extending from the sea bed to the emergency shutdown valve (ESDV) on the installation.

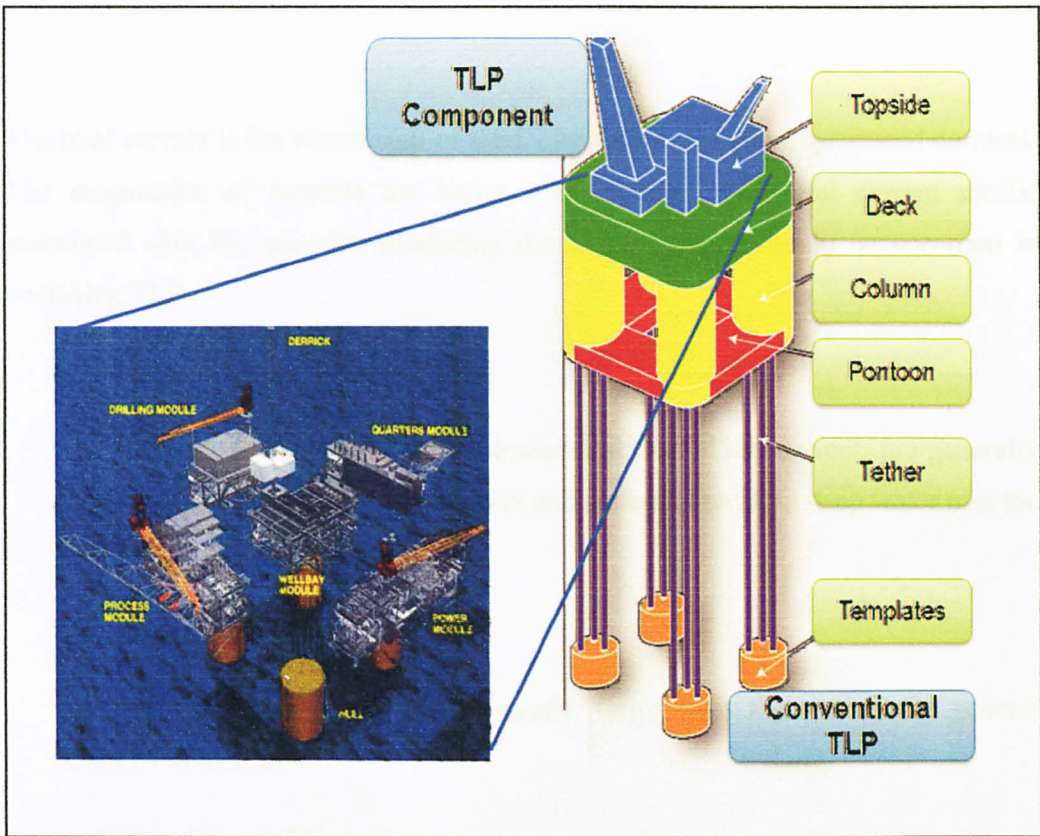


Figure 2.5: Component of Tension Leg Platform

Chianis, J., Poll, P., (1997, July) studies the advantages of TLP are

- Allows surface wellheads (dry tress)
- Drilling and work over capability
- Improved motion stability
- Experienced based cost and schedule data
- Reduced schedule in deepwater
- Large deck area. If required
- Large production capacity, if required
- Cost competitive with other deepwater system (for same water depth, payload. schedule)

2.3 Current Loads

The total current is the vector sum of tidal, circulation and storm generated currents. The magnitudes of currents varies with location. The total current profile associated with the sea-state producing the extreme wave should be specified in designing TLP.

- Tidal Currents

Tidal currents are associated with astronomical tides. Tidal currents are generally stronger on broad continentals' shelves and generally weak in deep water past the shelf break.

- Circulation Currents

Circulation currents are relatively steady, large scale features of the general oceanic circulation.

- Storm generated Currents

This current caused by the wind stress and atmospheric pressure gradient throughout the storm. The speed is depending on storm strength and meteorological characteristic such as bathymetric configuration and water density profile.

2.4 Linear Airy Wave Theory

Airy theory also called sinusoidal wave theory which is the simplest and most useful in the small amplitude wave theory. The assumption that wave height is smaller than wave length is taken for this theory to allow free surface boundary condition to be linearized. The wave height is dropped which are beyond the first order. As a result, it allows the free surface condition is satisfied at the mean water level, rather than at the oscillating free surface.

$$L = \frac{gT^2}{2\pi} \sqrt{\tanh \frac{4d\pi^2}{gT^2}} \quad (2.1)$$

$$K = \frac{2\pi}{L} \quad (2.2)$$

$$\omega = \frac{2\pi}{T} \quad (2.3)$$

$$\theta = kx - \omega t + \varepsilon n \quad (2.4)$$

$$u = \frac{\pi H}{T} \times \frac{\cosh ks}{\sinh kd} \times \cos \theta \quad (2.5)$$

$$u' = \frac{2H\pi^2}{T^2} \times \frac{\cosh ks}{\sinh kd} \times \sin \theta \quad (2.6)$$

2.5 Morison Equation

Morison Equation was developed by Morison, O'Brien, Johnson and Shaaf (1950) in describing the horizontal wave forces acting on a vertical pile which extends from the bottom through the free surface. Morison Equation assumes the forces to be composed of inertia and drag forces linearly added together. The components involve an inertia coefficient C_M and Drag Coefficient C_D with must be determined experimentally (Hydrodynamics of Offshore Structure, WIT Press, 1987. p.169).

There are two components forces which are exerted by the unbroken surface waves on a vertical pile which are inertia and drag force.

$$F = F_D + F_i \quad (2.7)$$

The concept of inertia force is where a water particle moving in a wave form carries along momentum with it. When the particle hit around the circular cylinder it accelerates and then decelerates. Inertia force equation:

$$F_i = \rho \times C_m \times \frac{\pi}{4} \times D^2 \times u' \cdot ds \quad (2.8)$$

Drag force is proportional to the square of the water particle velocity. The situation occurs in a steady flow where downstream side is fixed. The case where oscillatory flow is occur, drag force has to be ensure in the same direction as the velocity by substituting the absolute value of the water particle. Drag force equation:

$$F_D = \rho \times C_D \times \frac{D}{2} \times |u| \times u \cdot ds \quad (2.9)$$

2.6 Pierson-Moskowitz spectrum

Pierson-Moskowitz spectrum was developed in 1964 by Pierson and Moskowitz which propose a new formula for an energy spectrum distribution of a wind generated sea state base on similarity theory of Kitaigorodskii and more accurate recorded data. This spectrum had widely been used by ocean engineer as representative for water all over the world.

The P-M spectrum model is formulated by:

$$S(f) = \frac{\alpha g^2}{2\pi^4} \times f^{-5} \times \exp \left[-1.25 \times \left(\frac{f}{f_0} \right)^4 \right] \quad (2.10)$$

$$\omega_0^2 = \frac{0.161g}{H_s} \quad (2.11)$$

$$E = \frac{\omega}{2\pi} \quad (2.12)$$

2.7 Wave Profile

From the wave spectrum, the energy of the wave is translated to wave profile by calculating wave height by varies the time. Each time, t the height will be

different and from the plotted graph, maximum height of random wave can be determined.

Horizontal coordinate is fixed, elevation of the wave for time, t is determined by:

$$n(x, t) = \sum \frac{H(n)}{2} \cos[k(n)x - 2\pi f(n)t + \varepsilon(n)] \quad (2.13)$$

$$H(f) = 2 \times (2 \times S(f) \times \Delta f)^{-4} \quad (2.14)$$

2.8 Motion-Response Spectrum

Motion-response spectrum is theory used where a structure is move free in a wave and it may be critical near the resonance of the structure. The overall response of the platform is studied due to the design-wave spectrum. In this case, Pierson-Moskowitz spectrum is used. Total force is calculated for each frequency based on Pierson-Moskowitz spectrum. The formulas to get this motion response spectrum are:

$$S(f) = RAO^2 \times S(f) \quad (2.15)$$

$$RAO = \left[\frac{F_i / \frac{H}{2}}{\sqrt{(K - m\omega^2)^2 + (C\omega)^2}} \right] \quad (2.16)$$

CHAPTER 3

METHODOLOGY

3.1 Literature Survey

Research and investigation on Tension Leg Platform (TLP) and its responses due to current and wave had been done. A research had been collected through journals and books that available in internet and Universiti Teknologi Petronas Information Resources Centre. The main purpose of research is to determine the responses of the TLP in the form of hydrodynamic motion when it is subjected to environmental loads such as wave, current and wind. Besides that, a detailed survey of existing and under design or construction TLP had been gathered. The information and specification details of existent TLP had been gathered to make a comparison and to take the dimension for the modeling process.

3.2 Model selection of TLP

From the data and information that had been gathered the specification and dimension of the TLP will be compared. A conventional or classic TLP had been choose to make an analysis on the hydrodynamic responses. Ram Powell TLP had been chosen as the model TLP for this project.

3.2.1 Ram Powell Tension Leg Platform (TLP)

Ram Powell TLP will be used for tethers responses due wave and current. All the specification and parameter of the TLP will be used to analyst the responses. Ram-Powell TLP is located in Viosca Knoll area in the Gulf of Mexico. Ram-Powell unit encompasses eight Viosca Knoll Blocks- 867, 868, 911, 912, 913, 955, 956 and 957. This unit is own by shell.

This TLP had been installed on May 1997 and it had started operated the production on September 1997. Ran Powell is a 4 columns conventional TLP. The hull is made from steel. The parameter of Ram Powell as shown below

- Water depth, 980.2m
- Column Diameter, 21m
- Height of the column, 50m
- Dimension of the deck 75m x 75m
- Number of tethers, 12
- Length of tether, 959m
- Payload, 3500st

The dimension of the model should be efficient to be tested at the UTP offshore laboratory. The test will be conduct either at the wave tank with the dimension of 22.4m x 10.0m x 1.5m or wave flume with the dimension of 23.0m x 1.5m x 1.5m. When the dimension had been finalized then it will be fabricated using suitable material within the budget that had been allocated by the university.

3.3 Numerical Analysis

The analysis of the motion and tether forces of the platform subjected to random wave and current will be done by using Morison Equation. Morison Equation has the advantages of simplicity and has been used extensively to determine wave forces on small diameter members of offshore platform.

3.3.1 Wave Spectrum

Value from original field data such as significant wave height, H_s had been used for produced wave spectrum. Pierson Moskowitz spectrum had been used for the wave spectrum. Frequency had been taken from 0.005Hz to 0.255Hz with 0.010 interval had been taken to produce the spectrum.

$$S(f) = \frac{\alpha g^2}{2\pi^4} \times f^{-5} \times \exp\left[-1.25 \times \left(\frac{f}{f_c}\right)^4\right] \quad (3.1)$$

Then from the spectrum wave profile had been produce by using equation

$$n(x, t) = \sum \frac{H(n)}{2} \cos[k(n)x - 2\pi f(n)t + \varepsilon(n)] \quad (3.2)$$

3.3.2 Surge calculation

For surge calculation, the buoyancy, total pretension, surge stiffness, surge natural frequency and natural period had been determine first.

- Buoyancy of Column

$$No\ of\ Column \times \frac{\pi}{4} \times D^2 \times draft \times \rho \times g \quad (3.3)$$

- Buoyancy of Pontoon

$$No\ of\ pontoon \times w \times h \times l \times \rho \times g \quad (3.4)$$

- Total Buoyancy

$$Buoyancy\ of\ columns + Buoyancy\ of\ pontoons \quad (3.5)$$

- Total Pretension

$$Total\ Buoyancy - weight \quad (3.6)$$

- Pretension of each tether

$$S = \frac{Total\ Pretension}{Number\ of\ tethers} \quad (3.7)$$

- Diameter of pontoons , D_b

$$\frac{\pi D_b^2}{4} = w \times h \quad (3.8)$$

- Added mass Surge

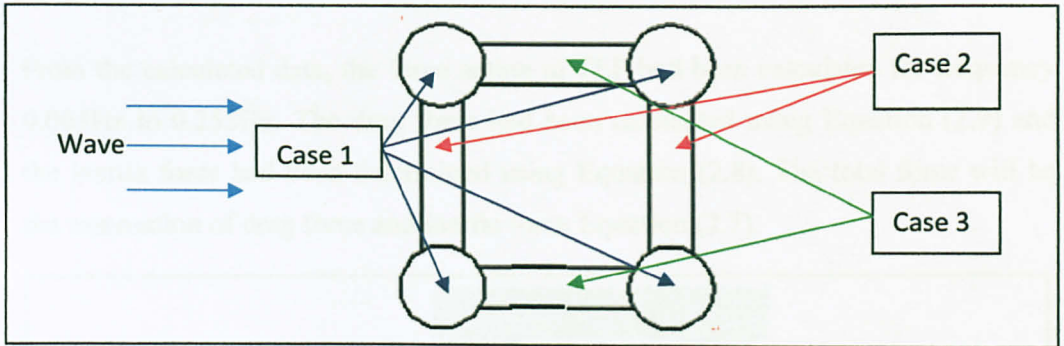


Figure 3.1: Added Mass For Surge

Case 1

$$No\ of\ columns \times \left(\frac{\pi}{4} \times D^2 \times draft \right) \times \rho \quad (3.9)$$

Case 2

$$No\ of\ pontoons \times (w \times h \times l \times \rho) \quad (3.10)$$

$$\text{No of pontoons} \times (w \times h \times l \times \rho) \quad (3.10)$$

Case 3

$$\text{No of pontoons} \times \left(\pi \times \frac{D_p^3}{12} \times \rho \right) \quad (3.11)$$

- Total Added Mass

$$\text{Added mass} + \text{Weight} \quad (3.12)$$

- Stiffness

$$K_{\text{surge}} = \frac{\text{Total Stiffness}}{\text{Length from seabed to pontoons}} \quad (3.13)$$

- Natural Frequency

$$\omega = \sqrt{\frac{\text{Surge Stiffness}}{\text{Total Added Mass}}}$$

(3.14)

- Natural Period

$$T_n = \frac{2\pi}{\omega} \quad (3.15)$$

From the calculated data, the force acting to TLP had been calculated for frequency 0.005Hz to 0.255Hz. The drag force had been calculated using Equation (2.9) and the inertia force had been determined using Equation (2.8). The total force will be the summation of drag force and inertia force Equation (2.7).

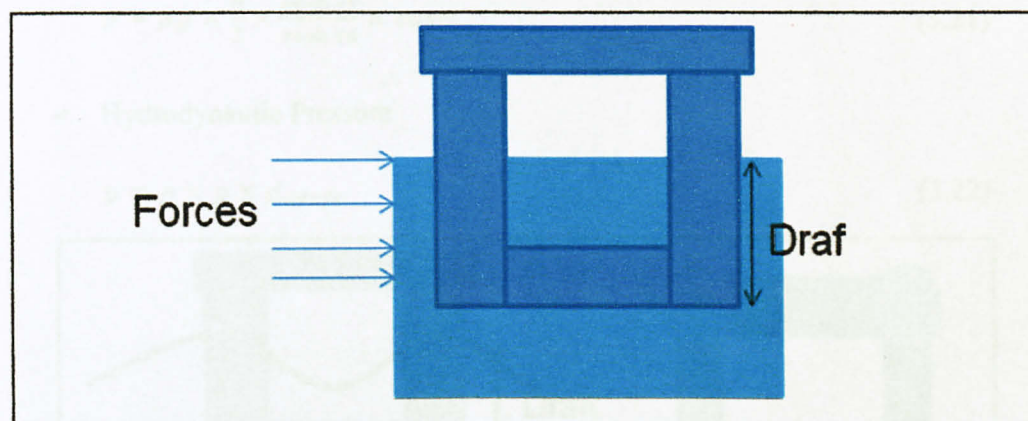


Figure 3.2: Surge Force Acting to the TLP

3.3.3 Heave Calculation

- Added mass heave for columns

$$\text{No of columns} \times \frac{\pi D^2}{12} \times \rho \quad (3.16)$$

- Added mass heave for pontoons

$$\text{No of pontoons} \times w \times h \times l \times \rho \quad (3.17)$$

- Total Mass Heave

$$M_{\text{Heave}} = \text{weight} + \text{added mass column} + \text{added mass pontoon} \quad (3.18)$$

- Heave Stiffness

$$K_{\text{Heave}} = \text{Tethers Stiffness} + \text{water plane area} \quad (3.19)$$

- Water plane area

$$\text{Water plane area} = 4 \times \frac{\pi D^2}{4} \times \rho \quad (3.20)$$

- Dynamic pressure

$$p = \rho g \times \frac{H}{2} \times \frac{\cosh ks}{\cosh kd} \times \cos \theta \quad (3.21)$$

- Hydrodynamic Pressure

$$p = \rho \times g \times d_{\text{draft}} \quad (3.22)$$

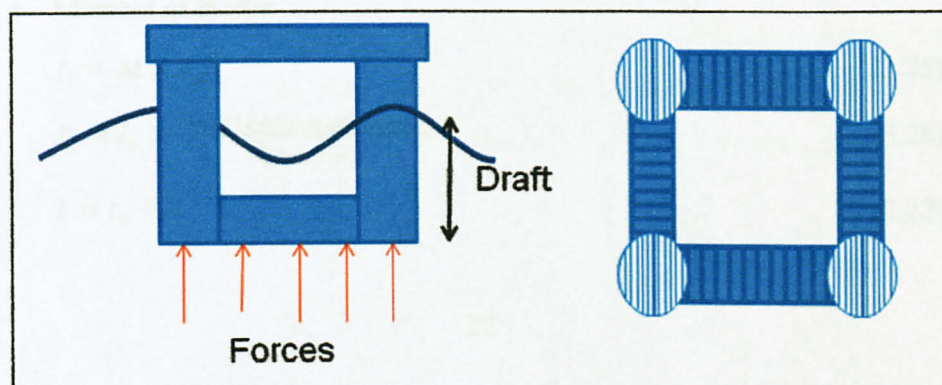


Figure 3.3: TLP subjected to vertical force

$$P = \text{Dynamic pressure} + \text{Hydrodynamic pressure} \quad (3.23)$$

- Force

$$Force_{\text{Heave}} = \text{Total pressure} \times \text{Area} \quad (3.24)$$

3.3.4 Pitch Calculation

Pitch is the moment of the structure. The force acting of the structure will be multiply with the length from the force acting to the center of gravity.

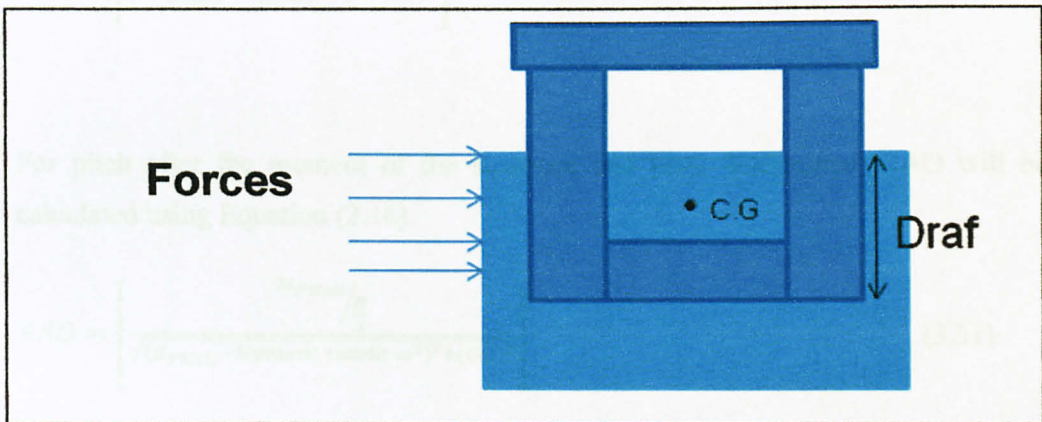


Figure 3.4: Total Moment Reaction to TLP

- Moment of inertia

$$I_1 = M \times R_z^2 \quad (3.25)$$

$$I_2 = I_1 \times \frac{M_{\text{total added mass (surge)}}}{M_{\text{platform}}} \quad (3.26)$$

$$I = I_1 + I_2 \quad (3.27)$$

3.3.5 Response-Amplitude Operator (RAO) calculation

Response-amplitude Operator is written relating the dynamic motion of the structure to the wave forcing on the structure. After the total force for surge had been determined, then RAO will be calculated using Equation (2.16).

$$RAO = \left[\frac{F_{Surge} / \frac{H}{2}}{\sqrt{(K_{Surge} - M_{Surge} \omega^2)^2 + (C\omega)^2}} \right] \quad (3.29)$$

For Heave, the after the total pressure had been calculated the RAO for heave been determined using Equation (2.16)

$$RAO = \left[\frac{P_{Heave} / \frac{H}{2}}{\sqrt{(K_{Heave} - M_{Heave} \omega^2)^2 + (C\omega)^2}} \right] \quad (3.30)$$

For pitch after the moment of the structure had been determined, RAO will be calculated using Equation (2.16)

$$RAO = \left[\frac{M_{Pitch} / \frac{H}{2}}{\sqrt{(K_{Pitch} - Moment\ Inertia\ \omega^2)^2 + (C\omega)^2}} \right] \quad (3.31)$$

3.3.6 Responses (Surge, Heave, Pitch) Spectrum

After all the RAO of the motion (surge, heave and pitch) had been determined, the responses spectrum for the three motion been determined by using Equation (2.15). When the responses spectrum had been plotted, then the responses profile will be determined using Equation (3.13)

3.3.7 Calculation for Different Current.

Then the effect of current will be considered. For surge, current will be added to the drag force in the Equation (2.9) and the equation with current as Equation (3.27). As the total forces in surge changes with current the moment had also changed with current.

$$F_D = \rho \times C_D \times \frac{D}{2} \times |u + i| \times u + i . ds \quad (3.32)$$

3.3.8 Results and Discussion.

3.4.1 Model scale down.

When the responses profile for surge, heave and pitch for various current speed had been determined. Then the different responses will be analyzed and compared.



Figure 3.3: Model testing dimension.

3.4 Experimental Analysis

Model had been tested at wave flume with the dimension of 23.0m x 1.5m x 1.5m. Prior to model testing the model had been scale down 1:200. The model had been fabricated using Perspex. Model had been tested by using regular wave generated by wave generator. The water depth is 100cm and the wave height is 0.05m. During this model testing, the responses will be recorded. The x-direction (surge) had been determined and z-direction (pitch) had been neglected for experiment because the responses are very small.

3.4.1 Model scale down.

From the actual dimension, by scaled down 1:200 the model for testing had been prepared. This dimension had been used so that a model test can be done in wave flume with 23.0m x 1.5m x 1.5m dimension. Refer to Figure 3.5 for details.

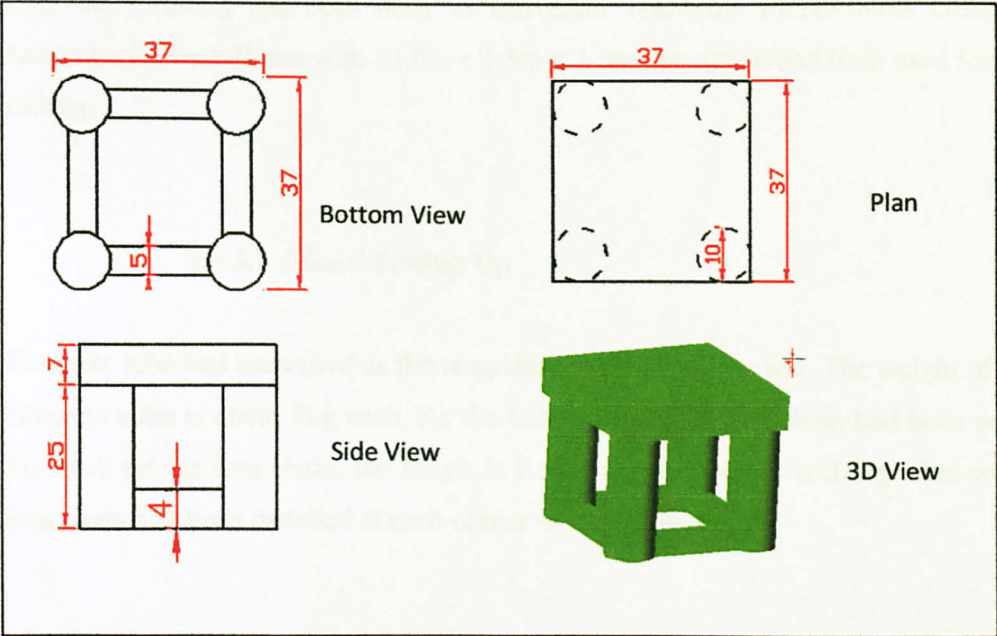


Figure 3.5: Model testing dimension

3.4.2 Model Fabrication

For the model fabrication Perspex had been used as the material for the model. The cost for the model is RM 310.00. The weight of the model is 2Kg. The model is water tight mean that it floats in the water.

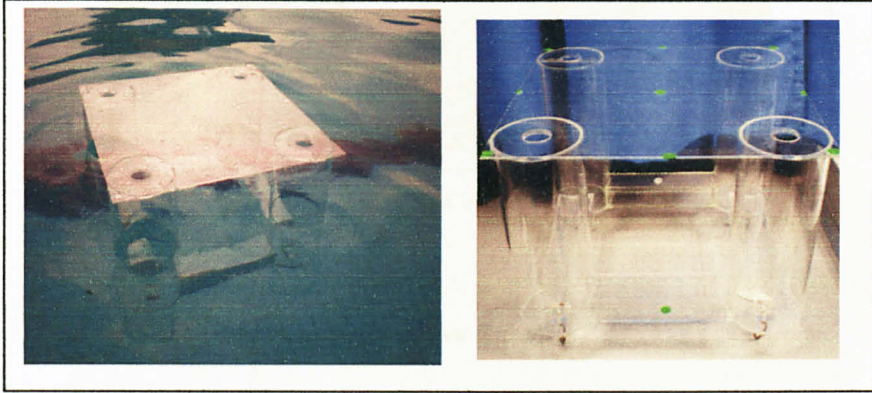


Figure 3.6: Fabricated model testing

3.4.3 Laboratory Model Testing

Laboratory testing had been done in Universiti Teknologi PETRONAS Offshore Laboratory. Wave flume with 23.0m x 1.5m x 1.5m dimension had been used for the testing.

3.4.3.1 Model Setting Up

Concrete tube had been used as the template or anchor for the test. The weight of the concrete cube is about 8kg each. As the tethers, 4 sets of iron chain had been used. For each set the iron chain, the length is 0.50m and the weight is 0.5kg. One set of iron chain had been installed at each corner of the column.



Figure 3.7: Model set up in the wave flume

3.4.3.2 Position in the wave flume

Then the model had been placed in the wave flume. Water had entered the wave flume and the water depth is set for 1m depth.

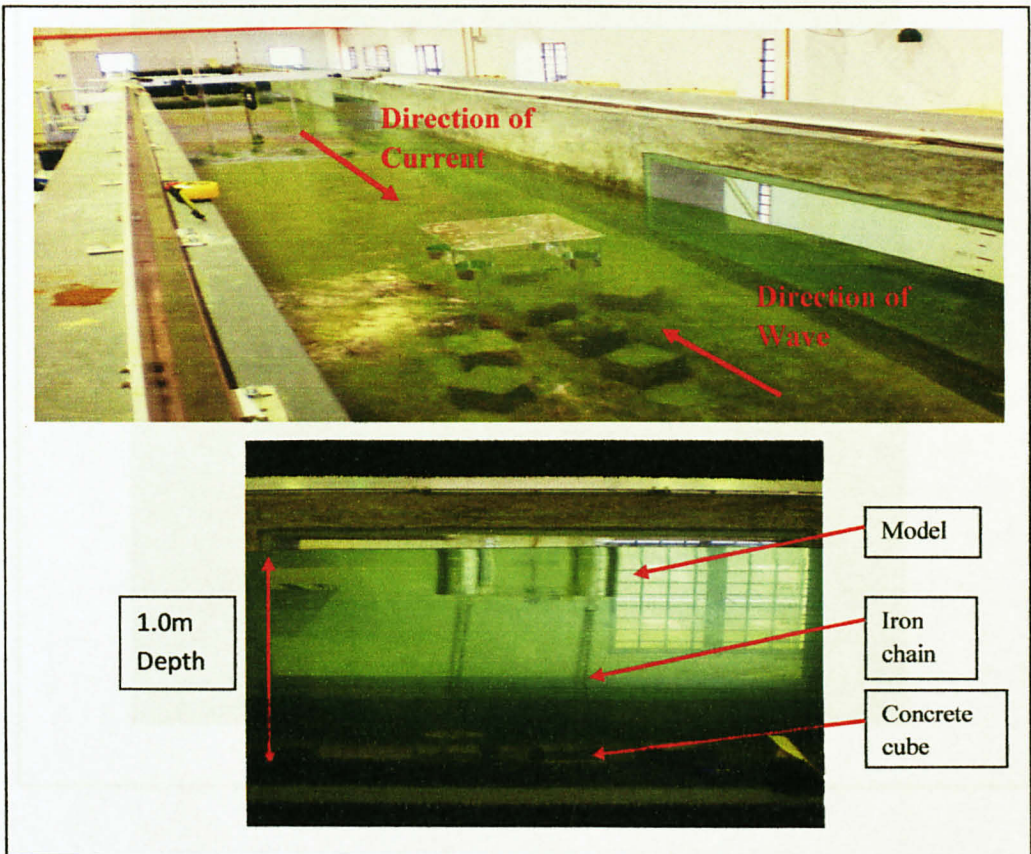


Figure 3.8: Position of the model in the wave flume

3.4.3.3 Start the experiment

When the model had been set up and the wave flume had been full with 1m depth of water. Then the wave generator had been operated. During the experiment, video had been taken to record the responses of the model. The experiment had been done for 0.05m wave height and varies frequency (0.25Hz, 0.35Hz and 0.45Hz).

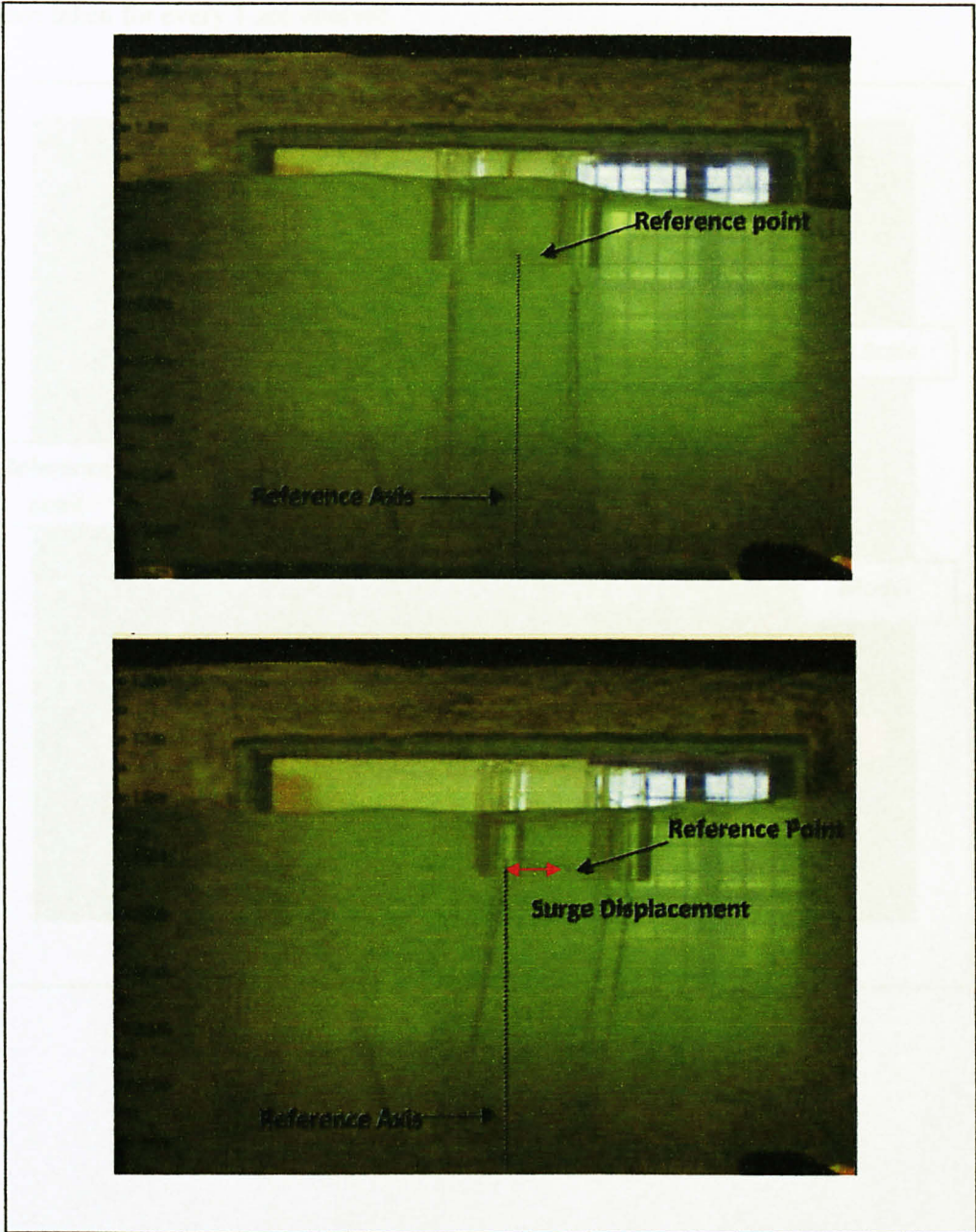


Figure 3.9: Model testing movement during the experiment

3.4.3.4 Responses Analysis

After the experiment had been completed the video recorded will be analyzed to determine the surge responses of the model. Only the surge (x-direction) responses had been considered for this experiment because the wave generated is regular wave and the heave responses are very small and can be neglected. The responses had been taken for every 1 sec interval.

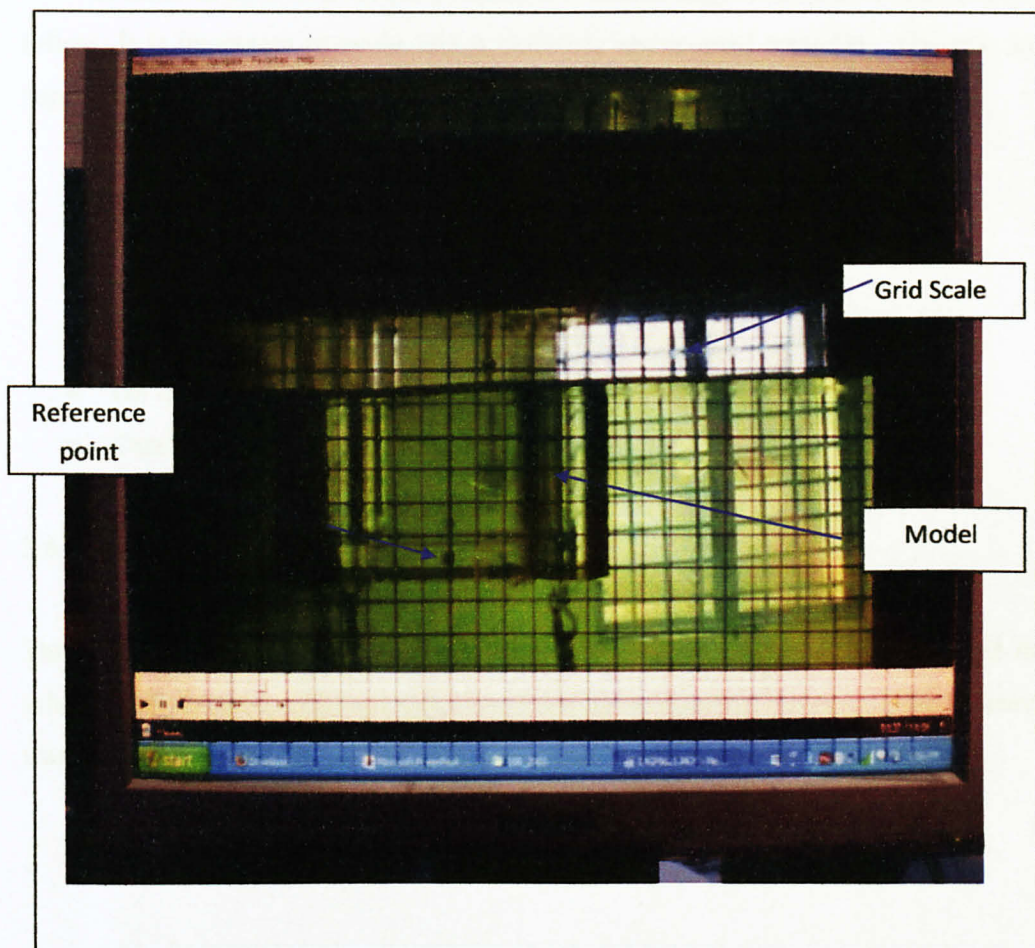


Figure 3.10: Calculating the laboratory model responses

3.5 Health safety and environment aspect.

Offshore laboratory has been a place where all the testing of the model studies as well as to visualize wave and current reaction. It is important to have better understanding about those things. It will lead to the best researches done where it supported by experimental result and data.

In order to enter and conduct experiment and testing, HSE requirement must be follow. It is important to avoid any accident or unexpected tragedies. The rule and regulation that someone must follow are;

- Obey all instruction given by the technicians or lecturer.
- Full covered shoes must be worn at all time.
- Do not touch any equipment control without permission.
- Do report to the technician if there is unusual thing.
- Do report to the technician if there is an accident happened.
- Careful during adjust the model in the water.

3.6 Project schedule

This project was followed the schedule that was planned earlier. By followed the schedule the project milestone can completed per scheduled. As results this research was completed in the time frame that was given by the university. (Appendix I)

3.7 Flow diagram of the methodology

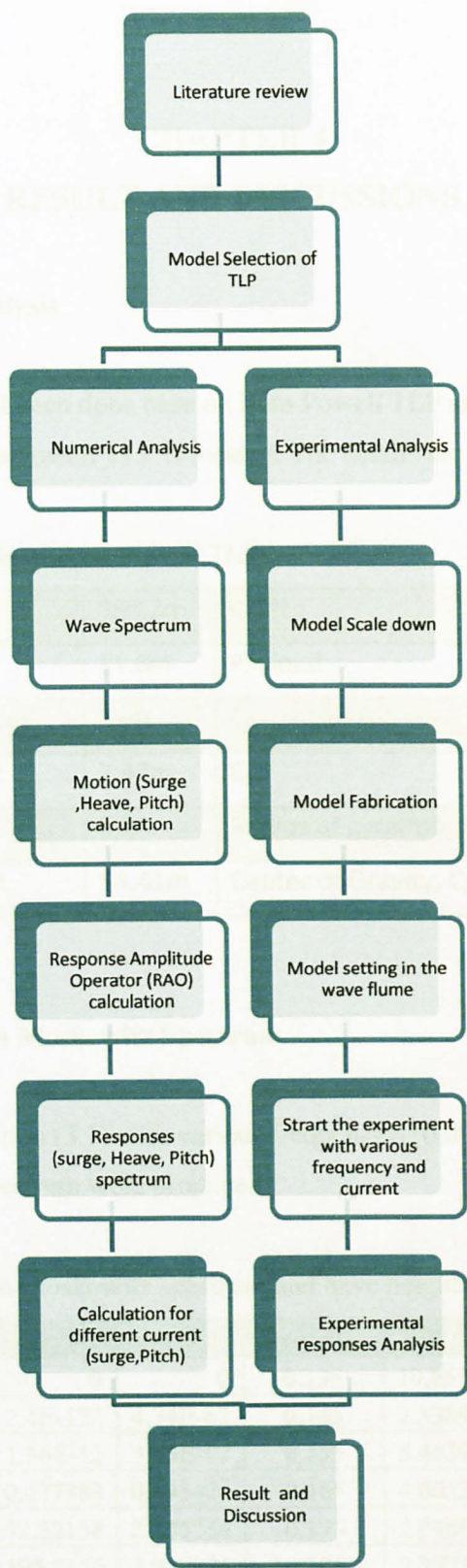


Figure 3.11: Flowchart of project Methodology

CHAPTER 4

RESULT AND DISCUSSIONS

4.1 Numerical analysis

Numerical analysis had been done base on Ram Powell TLP and sea-state at Gulf of Mexico where the Ram Powell TLP is located. The details are shown Table 4.1.

Table 4.1: Details of Ram Powell TLP

Water Depth	980.2m	Draft	25m
Hs	11.6m	Payload	3500st
Column Diameter	21m	C _D	0.65
Pontoon height	7.47m	C _M	1.60
Pontoon wide	8.23	Radius of gyration, R _z	38m
Pontoon length	54.41m	Center of Gravity, C _g	3m

4.1.1 Pierson Moskowitz Spectrum

By using Equation (3.1) with various frequencies (0.005Hz to 0.255Hz) the Pierson Moskowitz spectrum were produced.

Table 4.2: Pierson Moskowitz spectrum and wave height for each frequency

Frequency	S(f)	h(f)	Frequency	S(f)	h(f)
0.005	0	0	0.135	10.65751	0.923364
0.015	2.4E-122	4.34E-62	0.145	7.538999	0.776608
0.025	1.56E-12	3.53E-07	0.155	5.443933	0.659935
0.035	0.477383	0.195424	0.165	4.005206	0.566053
0.045	72.32158	2.405354	0.175	2.996952	0.489649
0.055	195.8156	3.957935	0.185	2.277102	0.426812
0.065	187.3866	3.871812	0.195	1.754341	0.37463

0.075	131.6825	3.245704	0.205	1.368758	0.330909
0.085	84.7334	2.603588	0.215	1.080283	0.293977
0.095	53.81677	2.074932	0.225	0.861627	0.262546
0.105	34.6515	1.664969	0.235	0.693896	0.235609
0.115	22.82289	1.351233	0.245	0.563804	0.212378
0.125	15.40891	1.110276	0.255	0.461873	0.192223

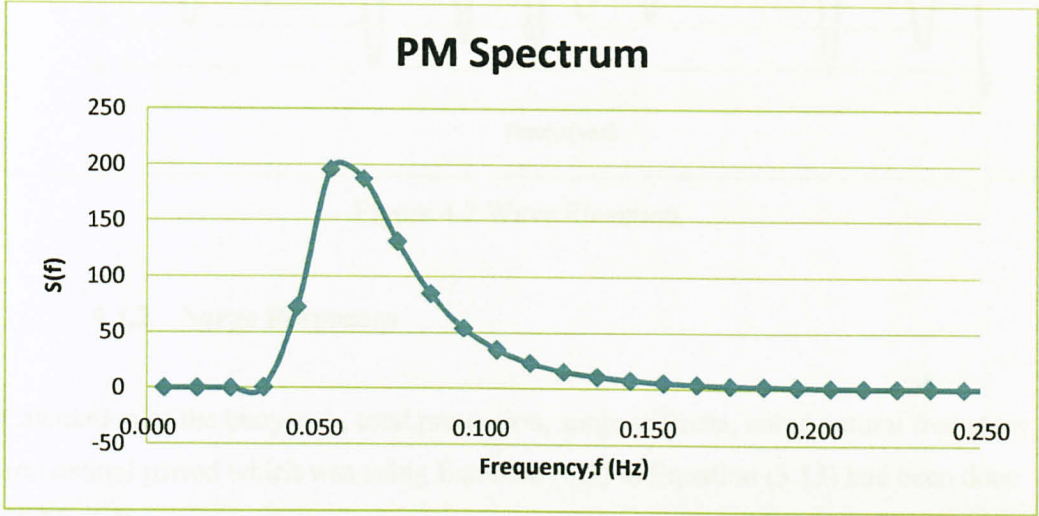


Figure 4.1: Graph Pierson Moskowitz Spectrum

From Figure 4.1 the $S(f)$ or energy density for this wave profile shown that the maximum value for this wave is 195.82 m^2 . This value is affected by significant wave height which is 11.6m . It affect through these equations.

$$\omega_0^2 = \frac{0.161g}{Hs} \tag{4.1}$$

$$E_0 = \frac{\omega_0}{2\pi} \tag{4.2}$$

From the wave analysis, Pierson Moskowitz Spectrum had been plotted. The shape of the spectrum is a bell shape. From the wave spectrum, the wave profile was calculated using Equation (3.2). The profile shows non linear fluctuation to the wave height due to random wave. With respect to time the elevation of wave had been done. The maximum wave elevation is about 7meter (Figure 4.2).

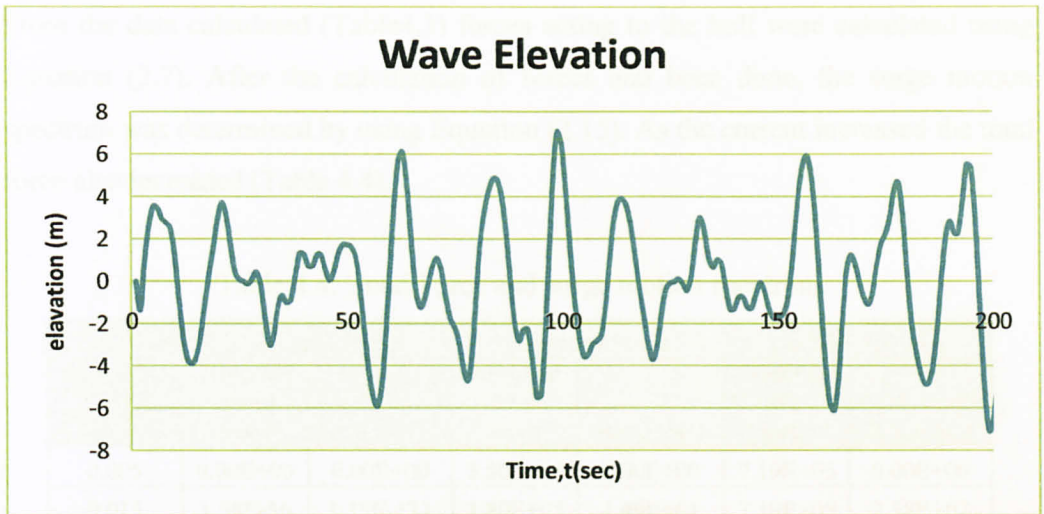


Figure 4.2 Wave Elevation

4.1.2 Surge Responses

Calculation of the buoyancy, total pretension, surge stiffness, surge natural frequency and natural period which was using Equation (3.3) to Equation (3.13) had been done (Table 4.3).

Table 4.3: Total added mass and Natural period of surge motion

Buoyancy of column,	326.01MN
Buoyancy of Pontoon	135.16MN
Total Buoyancy	461.16MN
Total Pretension	230.16MN
Pretension of each tethers	19.18MN
Diameter of pontoon	8.85m
Added mass- Case 1	33.24Mkg
Added mass- Case 2	6.8917Mkg
Added mass- Case 3	0.3734Mkg
Total Added mass	40.5065Mkg
Surge Stiffness	0.240103MN/m
Natural frequency	0.61221rad/sec
Natural Period	102.644sec

From the data calculated (Table4.3) forces acting to the hull were calculated using Equation (2.7). After the calculation of forces had been done, the surge motion spectrum was determined by using Equation (2.15). As the current increased the total force also increased (Table 4.4).

Table 4.4: Total Force and surge motion spectrum

Frequency	Current=0.00m/s		current=0.50m/s		Current=1.00m/s	
	Absolute total force	RAO² S(f)	Absolute total force	RAO² S(f)	Absolute total force	RAO² S(f)
0.005	0.00E+00	0.00E+00	1.80E+05	0.00E+00	7.19E+05	0.00E+00
0.015	1.58E-56	1.15E-121	1.80E+05	1.49E+01	7.19E+05	2.38E+02
0.025	2.39E-01	1.59E-12	1.80E+05	8.99E-01	7.19E+05	1.44E+01
0.035	1.49E+05	1.36E-01	4.31E+04	1.14E-02	6.55E+05	2.63E+00
0.045	4.51E+06	4.27E+01	2.12E+06	9.46E+00	3.53E+06	2.61E+01
0.055	7.48E+06	5.10E+01	4.56E+06	1.89E+01	1.14E+07	1.18E+02
0.065	1.54E+07	1.08E+02	4.79E+06	1.05E+01	5.61E+06	1.44E+01
0.075	1.17E+07	3.48E+01	1.59E+07	6.47E+01	3.26E+06	2.72E+00
0.085	1.45E+07	3.23E+01	1.27E+07	2.50E+01	1.13E+07	1.97E+01
0.095	1.18E+07	1.37E+01	1.27E+07	1.59E+01	1.14E+07	1.27E+01
0.105	1.23E+07	9.84E+00	1.25E+07	1.02E+01	9.77E+06	6.25E+00
0.115	4.86E+06	1.07E+00	8.25E+05	3.09E-02	6.25E+06	1.77E+00
0.125	9.79E+06	3.11E+00	9.17E+06	2.73E+00	8.99E+06	2.62E+00
0.135	6.01E+06	8.60E-01	4.01E+06	3.82E-01	7.62E+06	1.38E+00
0.145	1.98E+06	6.97E-02	7.17E+06	9.17E-01	4.33E+06	3.34E-01
0.155	3.54E+06	1.71E-01	1.07E+06	1.57E-02	6.65E+06	6.04E-01
0.165	1.91E+06	3.87E-02	5.37E+06	3.07E-01	4.71E+06	2.36E-01
0.175	4.94E+06	2.04E-01	3.56E+06	1.06E-01	2.17E+06	3.94E-02
0.185	3.95E+06	1.05E-01	4.24E+06	1.21E-01	1.29E+06	1.12E-02
0.195	1.57E+06	1.33E-02	2.20E+06	2.62E-02	2.80E+06	4.26E-02
0.205	1.49E+06	9.84E-03	3.46E+06	5.33E-02	3.62E+06	5.82E-02
0.215	4.39E+05	7.07E-04	1.31E+06	6.29E-03	1.77E+06	1.15E-02
0.225	1.62E+06	8.08E-03	9.33E+05	2.67E-03	1.99E+06	1.22E-02
0.235	1.55E+06	6.14E-03	1.53E+05	6.00E-05	4.00E+05	4.12E-04
0.245	4.11E+05	3.67E-04	5.74E+04	7.18E-06	2.74E+05	1.63E-04
0.255	9.56E+05	1.70E-03	9.52E+05	1.68E-03	9.61E+05	1.71E-03

From the surge spectrum graph (Figure 4.3), it shows the S (f) or energy density for the wave current 1.00m/s is higher follows by the wave with current 0.50m/s and finally wave with 0.00m/s current is the lowest energy density.

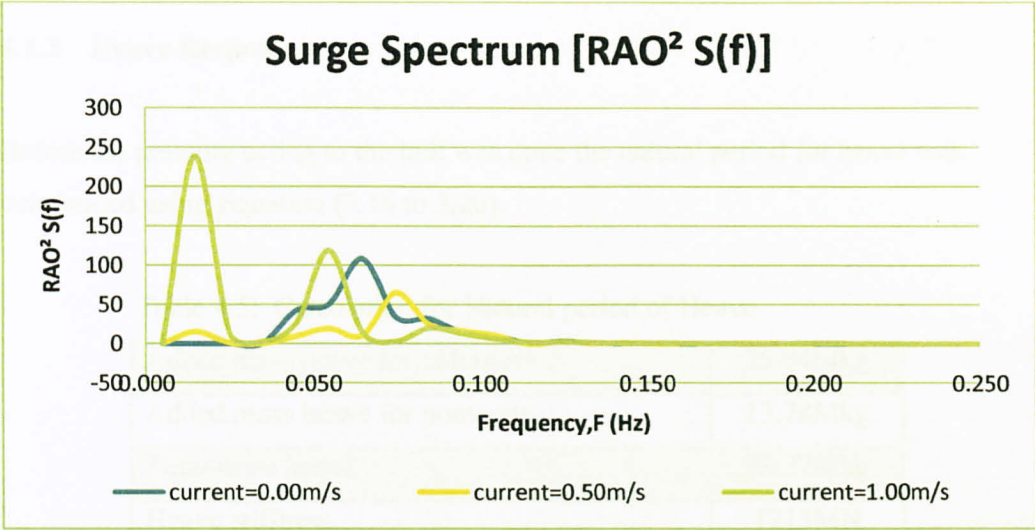


Figure 4.3: Graph of Surge Spectrum

After the surge spectrum was plotted, then the surge responses had been determined using Equation (3.2). From the Figure 4.4, the surge responses of the wave with no current were in range -3.5m to 3.5m. By adding 0.50m/s current the surge responses increase 8.6%. By adding 1.00m/s current the responses increase 17.1% from wave with no current.

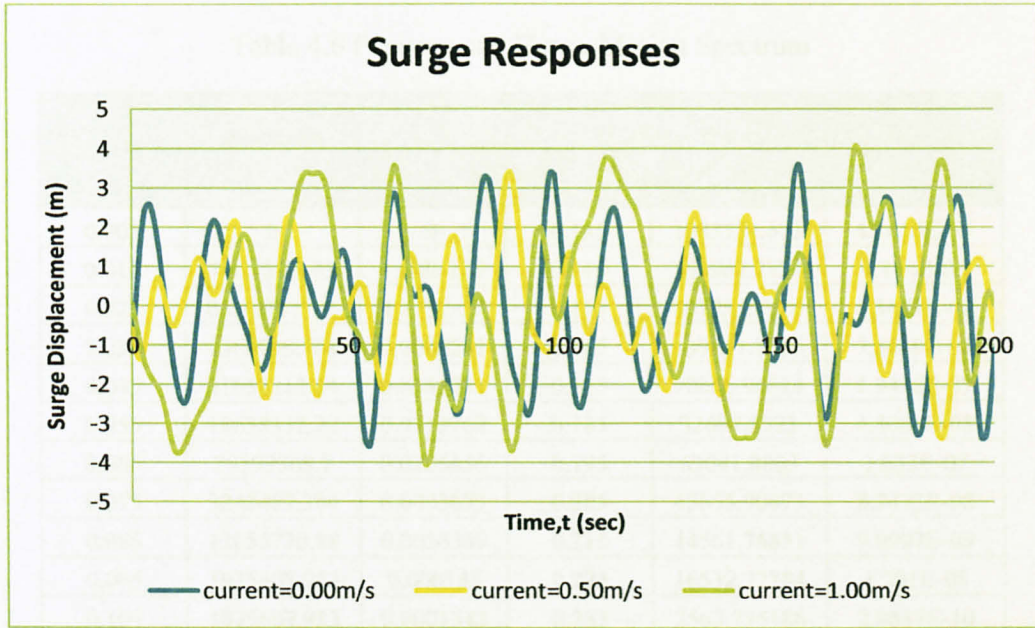


Figure 4.4: Graph of Surge Responses

4.1.3 Heave Responses

Before the pressure acting to the hull was done the natural period for heave was determined using Equation (3.16 to 3.20).

Table 4.5: Calculation for Natural period of Heave

Added mass heave for columns	35.94Mkg
Added mass heave for pontoons	13.78Mkg
Total mass heave	73.27Mkg
Heave stiffness	1213MN
Heave angular wave frequency	4.068rad/sec
Heave Natural period	1.544sec

From data calculated (Table 4.5), then pressure for the heave responses was determined using Equation (3.21-3.24). The heave motion spectrum was done using Equation (3.30) and Equation (3.2). As the current increased the total pressure also increased (Table 4.6)

Table 4.6 Pressure and Heave Motion Spectrum

Frequency	Absolute Total Pressure	RAO ² S(f)	Frequency	Absolute Total Pressure	RAO ² S(f)
0.005	0	0	0.135	1083734.673	4.3615E-05
0.015	7.02737E-55	1.68E-125	0.145	555962.2324	1.164E-05
0.025	0.050742795	8.775E-20	0.155	33725.24926	4.3485E-08
0.035	2560550.768	0.0002241	0.165	139341.8056	7.5449E-07
0.045	31652812.14	0.0343753	0.175	70066.96614	1.9412E-07
0.055	18638332.22	0.0119762	0.185	32697.6523	4.3068E-08
0.065	29199368.7	0.0295636	0.195	63041.8863	1.633E-07
0.075	3243487.304	0.0003673	0.205	45655.90473	8.7473E-08
0.085	12655770.88	0.0056349	0.215	14561.76831	9.0997E-09
0.095	1935607.953	0.000133	0.225	16532.22784	1.201E-08
0.105	1935607.953	0.0001343	0.235	2563.775186	2.9617E-10
0.115	20494141.91	0.0152159	0.245	3259.691415	4.9165E-10
0.125	495876.8445	9.014E-06	0.255	63041.8863	1.8911E-07

From the value of $RAO^2 S(f)$ (Table 4.6), heave spectrum were plotted for frequency 0.005Hz to 0.255Hz. The maximum value of the $S(f)$ or energy density for the wave is 0.033 which is at frequency 0.045Hz.

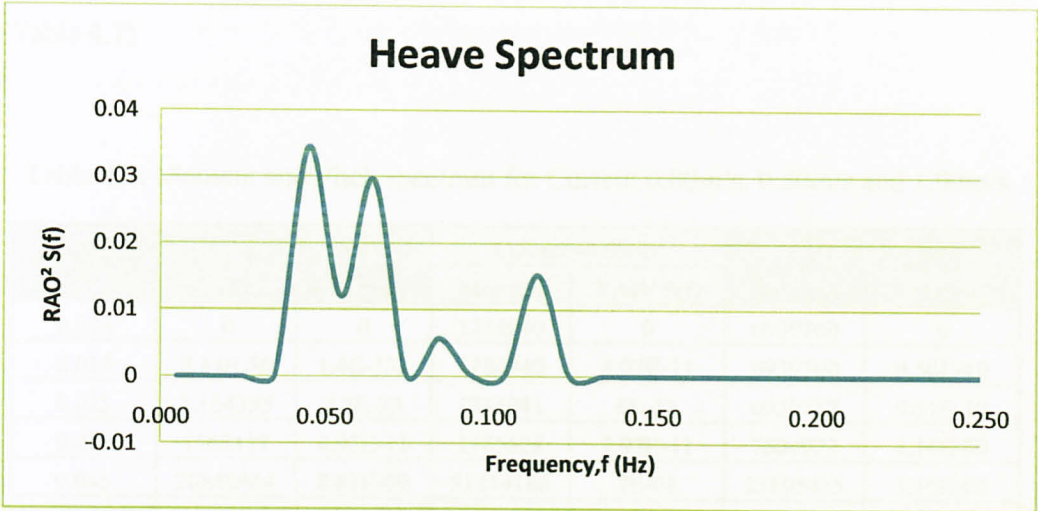


Figure 4.5 Graph of Heave motion Spectrum

Then the heave responses were calculated using Equation (3.2). The maximum heave response was 0.07m (Figure 4.6). From the numerical analysis the heave responses was normally at range 0.02m to 0.04m. The heave responses were very small. The tendon that in tension position was caused the heave motion is small. This is one of the advantages of TLP where the heave motion was small.

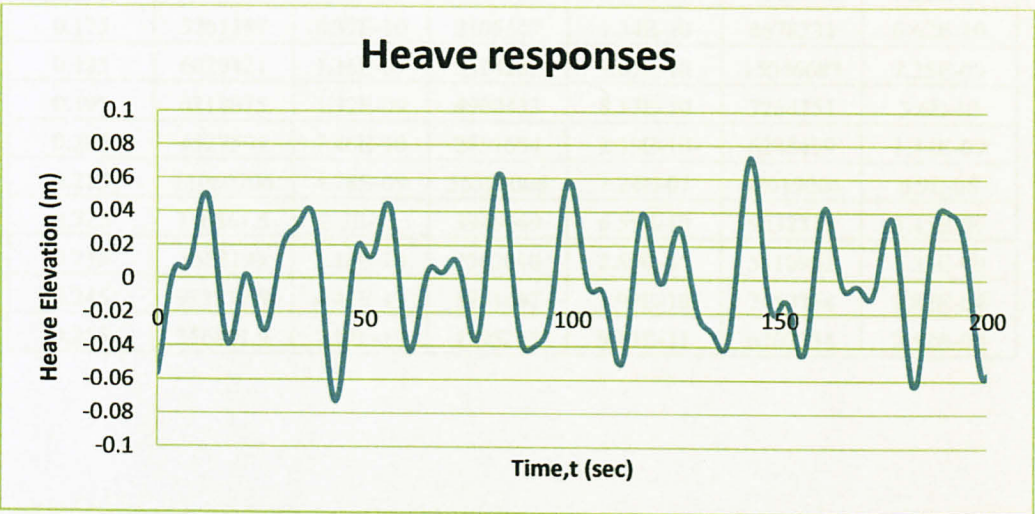


Figure 4.6 Graph of Heave motion Responses

4.1.4 Pitch Responses

Generally the pitch responses of TLP were related to the moment of inertia of the structure. The moment had been done using Equation (3.28). The pitch spectrum was calculated using Equation (3.31). As the current increase the moment also increase (Table 4.7)

Table 4.7: Moment and Pitch spectrum for Current 0.00m/s, 0.50m/s and 1.00m/s

Frequency	Current=0.00m/s		Current=0.50m/s		Current=1.00m/s	
	Moment	RAO ² S(f)	Moment	RAO ² S(f)	Moment	RAO ² S(f)
0.005	0	0	1734940	0	6939760	0
0.015	8.45E-56	1.4E-133	1734940	5.97E-11	6939760	9.56E-10
0.025	1.164385	2.7E-23	1734941	6E-11	6939762	9.61E-10
0.035	1565417	4.92E-11	1985628	7.92E-11	7604922	1.16E-09
0.045	20848664	8.82E-09	31419186	2E-08	23895935	1.16E-08
0.055	25936914	1.38E-08	58765777	7.1E-08	58115776	6.94E-08
0.065	58165045	7.06E-08	59922524	7.5E-08	69898735	1.02E-07
0.075	61965634	8.16E-08	54558322	6.33E-08	80554579	1.38E-07
0.085	33783236	2.48E-08	83492454	1.51E-07	10668960	2.47E-09
0.095	76789621	1.31E-07	2068480	9.51E-11	23113341	1.19E-08
0.105	61951030	8.76E-08	45850565	4.8E-08	47739668	5.2E-08
0.115	43154018	4.38E-08	8679543	1.77E-09	60637338	8.65E-08
0.125	4810043	5.62E-10	31902716	2.47E-08	42980980	4.49E-08
0.135	17907125	8.08E-09	4916585	6.09E-10	16301624	6.7E-09
0.145	27411679	1.97E-08	28975550	2.2E-08	30279845	2.4E-08
0.155	14164007	5.5E-09	7123107	1.39E-09	1102757	3.33E-11
0.165	13585986	5.3E-09	3174535	2.89E-10	1566276	7.05E-11
0.175	5261187	8.37E-10	2105547	1.34E-10	4678233	6.62E-10
0.185	6020421	1.16E-09	5324287	9.07E-10	15046683	7.25E-09
0.195	6218675	1.32E-09	4900433	8.17E-10	3254351	3.6E-10
0.205	4527591	7.46E-10	2451604	2.19E-10	6288499	1.44E-09
0.215	11060706	4.78E-09	56324008	1.24E-07	42019066	6.9E-08
0.225	736561.5	2.3E-11	3946569	6.59E-10	9032317	3.45E-09
0.235	1583199	1.16E-10	2502010	2.89E-10	5410952	1.35E-09
0.245	933817.9	4.41E-11	1951667	1.93E-10	7459754	2.82E-09
0.255	356891.9	7.14E-12	1295257	9.41E-11	6703231	2.52E-09

From the value of $RAO^2 S(f)$ (Table 4.7), pitch spectrum were plotted for frequency 0.005Hz to 0.255Hz (Figure 4.7). The maximum value of the $S(f)$ or energy density for the wave with no current was $1.31E-07$ at frequency 0.095Hz. For wave with 0.50m/s current the maximum value of energy density was $1.51E-07$ at frequency 0.085Hz. For wave with 1.00m/s current, the maximum value of energy density which was $1.38E-07$ at 0.075Hz

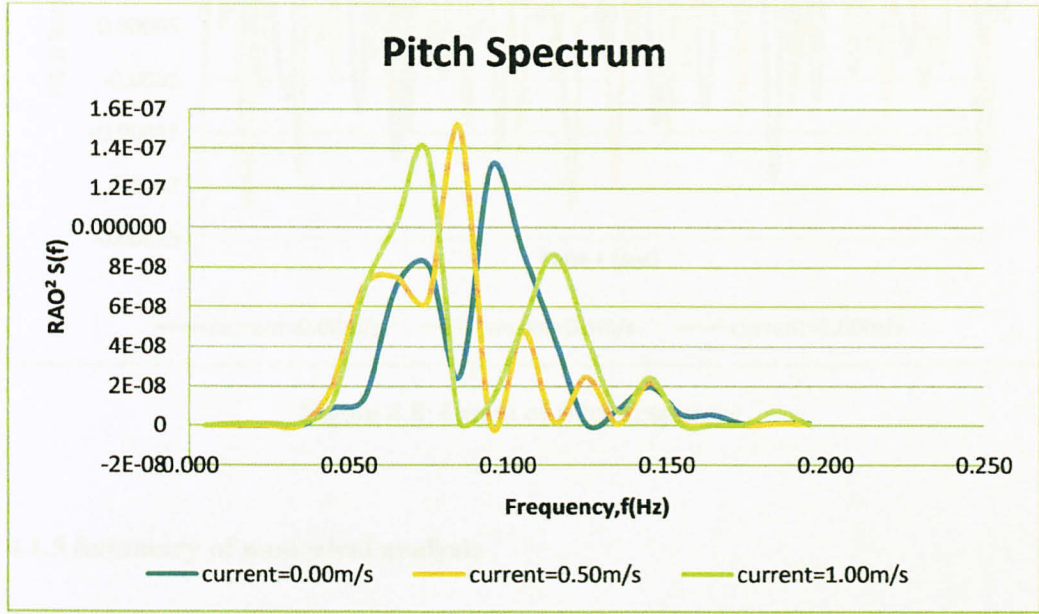


Figure 4.7: Graph of pitch motion spectrum

After the pitch spectrum was plotted, then the pitch responses were determined using Equation (3.2). The maximum pitch response of the wave with no current was 0.000200radian. The maximum pitch responses of wave with 0.50m/s current was 0.000215radian. The maximum pitch response of wave with 1.00m/s current was 0.000225radian. By adding 0.50m/s current, the surge responses increase 7.5%. By added 1.00m/s current, the responses increase 12.5% from wave with no current (Figure 4.8).

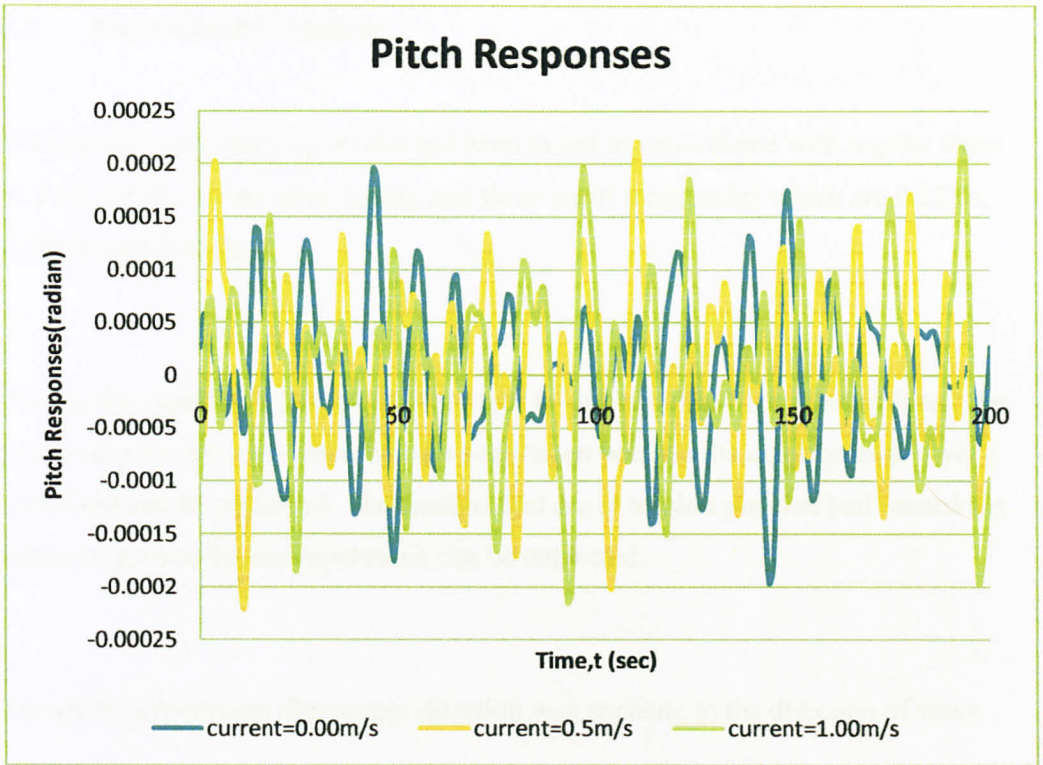


Figure 4.8: Graph of pitch responses

4.1.5 Summary of numerical analysis

From the numerical analysis of the surge, heave and pitch responses, the summary are shown in Table 4.8.

Table 4.8: Summary from numerical Analysis

Motions	Responses with no Current	Current=0.50m/s	Current=1.00m.s
Surge	Max=3.50m	8.6%	17.1%
Heave	Max=0.07m	-	-
Pitch	Max=0.00018rad	7.5%	12.5%

4.2 Experimental Analysis

For experimental analysis, model had been tested in wave flume with regular wave in 1.0m depth, 0.05m wave height, and three set of frequencies which are 0.25Hz, 0.35Hz, and 0.45Hz.

During the experiment, the surge responses (x-direction) had been determined. The heave responses (z-direction) had not been taken because the displacement is very small and can be neglected. The tendons that are in tension position had caused the heave responses for the experiment can be neglected.

For all the experiment the current direction was apposite to the direction of wave.

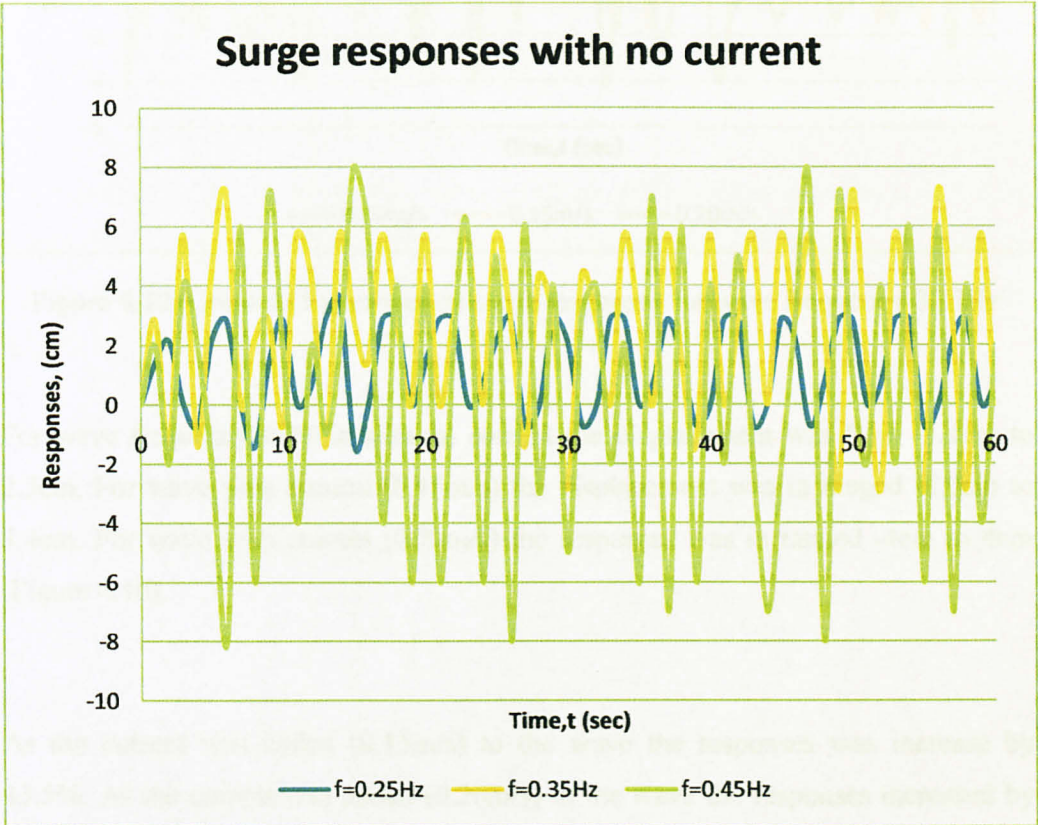


Figure 4.9: Surge responses for wave with no current

.The surge responses of the regular wave with no current were plotted (Figure 4.9). Frequency 0.25Hz, the maximum response was 2.1cm. For frequency 0.35Hz the maximum frequency was 6.6cm. For frequency 0.35Hz the maximum response was 10.6cm.

As the frequency increased the responses were increased.

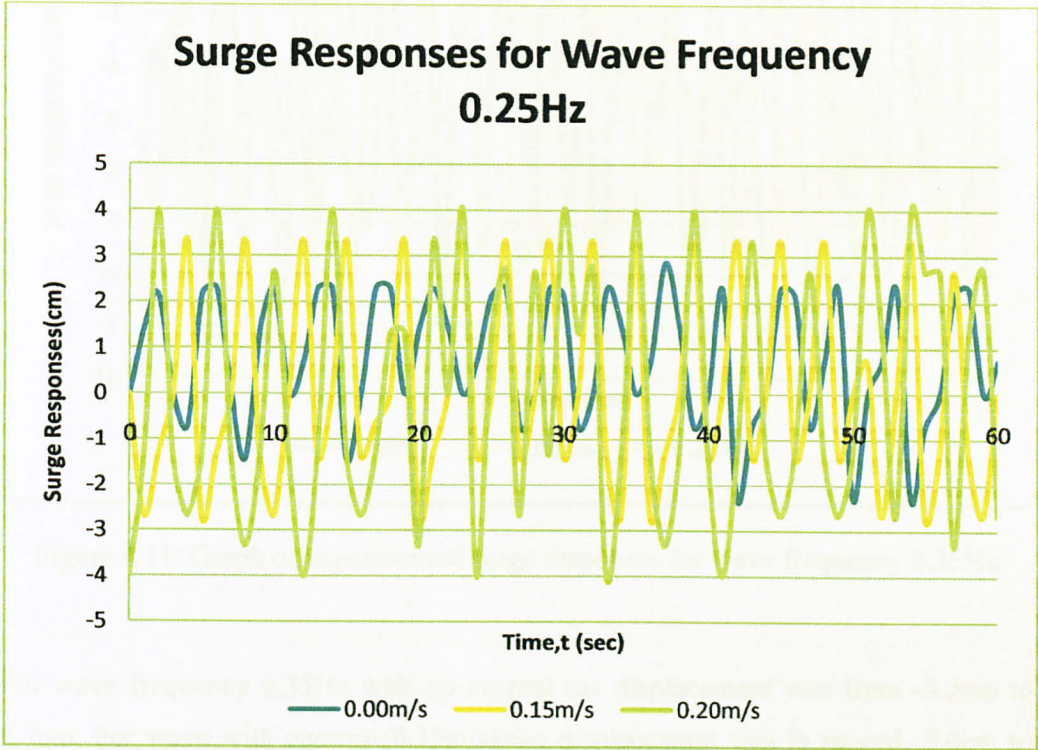


Figure 4.10: Graph of Experimental surge responses for wave frequency 0.25Hz

For wave frequency 0.25Hz with no current the displacement was from -1.4cm to 2.3cm. For wave with current (0.15m/s) the displacement was in ranged -2.7cm to 3.4cm. For wave with current (0.20m/s) the responses was in ranged -4cm to 4cm (Figure 4.10).

As the current was added (0.15m/s) to the wave the responses was increase by 43.5%. As the current was added (0.20m/s) to the wave the responses increased by 59.4%.

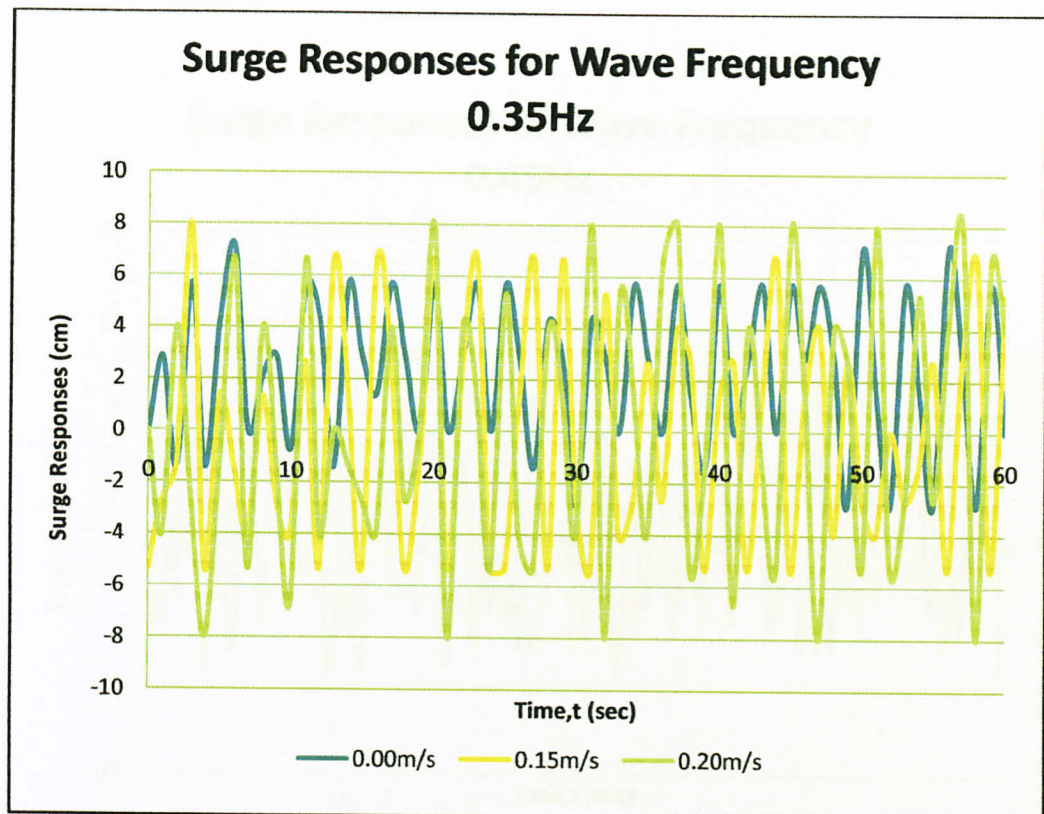


Figure 4.11: Graph of experimental surge responses for wave frequency 0.35Hz

For wave frequency 0.35Hz with no current the displacement was from -3.3cm to 5.7cm. For wave with current (0.15m/s) the displacement was in ranged -5.6cm to 6.7cm. For wave with current (0.20m/s) the responses was in ranged -8.0cm to 8.0cm (Figure 4.11).

As the current was added (0.15m/s) to the wave the responses was increase by 16.6%. As the current was added (0.20m/s) to the wave the responses increased by 39.2%.

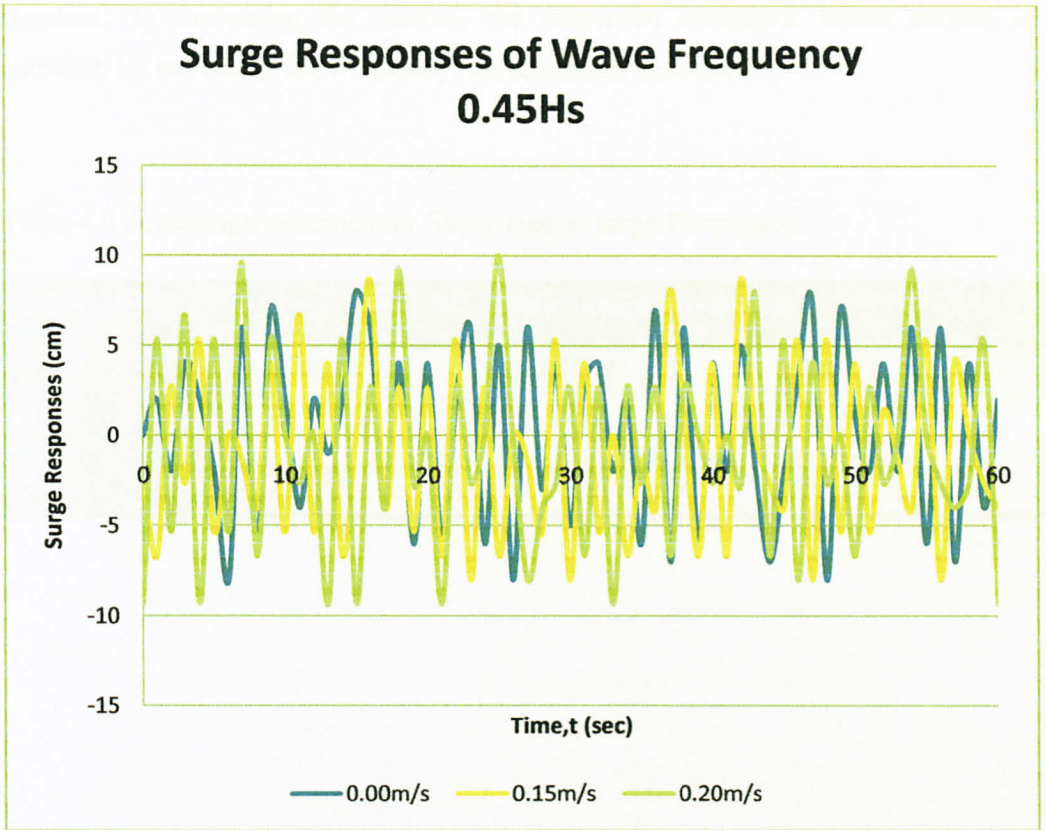


Figure 4.12: Graph of experimental surge responses of wave frequency 0.45Hz

For wave frequency 0.45Hz with no current the displacement was from -6.8cm to 7.6cm. For wave with current (0.15m/s) the displacement was in ranged -8.0cm to 8.7cm. For wave with current (0.20m/s) the responses was in ranged -9.3cm to 10.0cm (figure 4.12).

As the current was added (0.15m/s) to the wave the responses was increase by 14.0%. As the current was added (0.20m/s) to the wave the responses increased by 31.6%.

Summary results from the experiment are shown in Table 4.8. When frequency is constant, by increasing the current, the responses increased. When current is constant, by increasing the frequency, the responses decreased.

CHAPTER 5

Table 4.8 Percentage increment or Experimental surge Responses.

Current (m/s)	Percentage Increment		
	0.25 Hz	0.35Hz	0.45Hz
0.15	43.5%	16.6%	14.0%
0.20	59.4%	39.9%	31.6%

From the experimental analysis, the surge response with no current (current = 0.00m/s) was 0.00%. When the surge was added with 0.15m/s current, the surge response increased by 43.5%. When the surge was added with 0.20m/s current, the surge response increased by 59.4%.

From experimental surge analysis, the maximum surge response was 0.07m. Current did not affect the response. This was because the current was moving horizontally while surge direction of pressure was acting vertically on the TLP.

From experimental surge analysis, the surge response with no current (current = 0.00m/s) was 0.00% radial. By adding 0.15m/s current, the surge response was increased by 7.5%. By adding 0.20m/s current, the surge response was increased by 12.5%. The surge of TLP was small but was the motion was sustained by performance of motion.

From the experimental analysis, it showed that current affected the surge response. For frequency 0.25Hz was 43.5% for 0.15m/s and 59.4% for 0.20m/s. For 0.35Hz the response was 16.6% for 0.15m/s and 39.9% for 0.20m/s. While for 0.45Hz the surge responses were 14.0 for 0.15m/s and 31.6% for 0.20m/s. The surge motion for experimental analysis could be neglected because the value was too small.

CHAPTER 5

CONCLUSION AND RECOMMENDATION

5.1 Conclusion

From the numerical analysis, the maximum surge response with no current was 3.5m. When the wave was added with 0.50m/s current the surge responses increase by 8.6%. When the wave was added with 1.00m/s currents the surge responses increase by 17.1%.

From numerical heave analysis, the maximum heave response was 0.07m. Currents did not affect the responses. This was because the current was moving horizontal while heave force or pressure was acting vertically to the TLP.

From numerical pitch analysis, the pitch responses with no current (current=0.00m/s) was 0.0002radian. By adding 0.50m/s current, the pitch responses were increased by 7.5%. By adding 1.00m/s current, the pitch responses were increased by 12.5%. The pitch of TLP was small because the motion was restrained by pretension of tendons.

From the experimental analysis, it showed that current affected the surge responses for frequency 0.25Hz was 43.5% for 0.15m/s and 59.4% for 0.20m/s. For 0.35Hz the responses were 16.6% for 0.15m/s and 39.9% for 0.20m/s. While for 0.45Hz the surge responses were 14.0 for 0.15m/s and 31.6% for 0.20m/s. The heave motion for experimental analysis could be neglected because the value was too small.

Current should be taken into account while designing TLP because it has an effect on the motion responses especially surge motion where it is highly affected. As shown in both numerical and experimental analysis by adding certain value of current the responses also change.

From experimental analysis when frequency is constant, by increasing the current, the responses increased. While, when current is constant, by increasing the frequency, the responses decreased.

5.2 Recommendation

For the continuation of this project, comparison can be made on motion responses of various type of Tension Leg Platform (TLP) such as Conventional TLP, SeaStar TLP and Moses TLP. This comparison will show which type of TLP has less motion.

From this project there are several aspects that can be improved for future research especially in laboratory model testing. For this project equipment to determine the responses such as load cell is not available. This load cell can give more accurate results compare to manual calculation that had been made on this project.

Besides that, for continuation of this project, it will be better if the model testing can be made with irregular wave. As the real condition in the ocean where the wave is irregular so that more motion can be observe.

In the future for better comparison the numerical responses can be compared with software analysis such as SACS. This will give more accurate results on comparison the result.

Several items for the numeral analysis are taken base on other detail are available from other TLP. Details of Ram Powell TLP (e.g. radius of gyration and center of gravity) are needed to get a more accurate numerical analysis.

REFERENCESS

- Chakrabarti, S.K. (1987). *Hydrodynamic of Offshore Structure*. Eastbound: WIT Press.
- Chakrabarti, S.K. (1994). *Offshore Structure Modelling*. Singapore: World Scientific.
- Mather, A. (2000). *Offshore Enginerring an Introduction*. Great Britain: Witherby.
- Yong Bai. (2003). *Marine Structural Design*. UK: Elsevier.
- Adzerin, R., Benaroya, H. (1999). Response of a tension leg platform to stochastic wave forces. *Journal of Probabilistic Engineering Mechanics*, 14, 3-17.
- Ahmad, S. (1995). Stochastic TLP responses under long crested random sea, *Journal of computer and Structures* 61, 975-993.
- Chandasekaran, S., Jain, A.K., Chandak, N.R. (2004). Influence of hydrodynamic coefficient in the response behaviour of triangular TLPs in regular wave. *Journal of Ocean Engineering* 31, 2319-2342.
- Chianis, J., Poll, P., (1997, July). Studies clear TLP cost, Depth Limit Misconception. *Offshore*, 42-22.
- Pallanich, J. (2008, January). Extending the TLP brand. *Offshore*, 38-39.
- Patel, M.H., Witz, J.A., (1991). *Compliant Offshore Structures*. Great Britain: Butterworth-Heinemann

APPENDIXES

APPENDIX I: Project Schedule (Gantt Chart)

APPENDIX II: Details of Ram Powell TLP

APPENDIX III: Surge Calculation (Microsoft Excel)

APPENDIX IV: Heave Calculation (Microsoft Excel)

APPENDIX V: Pitch Calculation (Microsoft Excel)

APPENDIX I: Project Schedule (Gantt Chart)

No.	Description	Weeks	1	2	3	4	5	6	7	8	9		10	11	12	13	14	15
		Dates	18-Jan	25-Jan	3-Feb	9-Feb	16-Feb	23-Feb	2-Mar	9-Mar	16-Mar	23-Mar	30-Mar	6-Apr	13-Apr	20-Apr	27-Apr	4-May
1	Project Research (continuation)																	
	Heave Motion Analysis																	
	Pitch Motion Analysis																	
	Current affect on Heave motion																	
	Current affect on pitch motion																	
	Preparatrion for progress report																	
	Preparation for poster presentation																	
	Preparation for Disertation report																	
	Preparation for Oral Presentation																	
2	Project laboratory Experiment																	
	Laboratory check-up																	
	Model Setting																	
	Experiment Trial run																	
	Experiment testing																	
	Data interpretation																	
	Model Analysis																	

 Completed
 Process
 Deliverables
 Mid-semester break

APPENDIX II: Details of Ram Powell TLP

The Ram Powell TLP is the first of its kind, approximately 125 miles from the Alabama and Georgia border, east of Mobile, Alabama. It is owned by Ram Powell TLP, LLC, and is the first TLP to be owned by the Alabama Department of Transportation. The TLP was built by the Alabama Department of Transportation in 1998, and is the first TLP to be built in the state.

The TLP was built by the Alabama Department of Transportation in 1998, and is the first TLP to be built in the state. It is the first TLP to be built in the state, and is the first TLP to be built in the state.

The TLP is a commercial pay toll with a length of 1.25 miles. It is the first TLP to be built in the state, and is the first TLP to be built in the state.

WELL TLP

The Well TLP is a commercial pay toll with a length of 1.25 miles. It is the first TLP to be built in the state, and is the first TLP to be built in the state.

WELL TLP

The Well TLP is a commercial pay toll with a length of 1.25 miles. It is the first TLP to be built in the state, and is the first TLP to be built in the state.

The Well TLP is a commercial pay toll with a length of 1.25 miles. It is the first TLP to be built in the state, and is the first TLP to be built in the state.

The Well TLP is a commercial pay toll with a length of 1.25 miles. It is the first TLP to be built in the state, and is the first TLP to be built in the state.

The Well TLP is a commercial pay toll with a length of 1.25 miles. It is the first TLP to be built in the state, and is the first TLP to be built in the state.

The Well TLP is a commercial pay toll with a length of 1.25 miles. It is the first TLP to be built in the state, and is the first TLP to be built in the state.

WELL TLP

The Well TLP is a commercial pay toll with a length of 1.25 miles. It is the first TLP to be built in the state, and is the first TLP to be built in the state.

WELL TLP

The Well TLP is a commercial pay toll with a length of 1.25 miles. It is the first TLP to be built in the state, and is the first TLP to be built in the state.

Ram Powell, Gulf of Mexico, USA


[Email Article](#)

[Print](#)

[Link To Us](#)

Ram Powell lies in the Viosca Knoll area in the Gulf of Mexico, approximately 125 miles south-east of New Orleans and around 80 miles south of Mobile, Alabama in water depths ranging from 2000 to 4000ft. The Ram Powell Unit, approved by the Minerals Management Service in June 1989, encompasses eight Viosca Knoll blocks - 867, 868, 911, 912, 913, 955, 956 and 957.

DRILLING

The discovery well was drilled on Viosca Knoll block 912 in May 1985, using the drillship Discoverer Seven Seas. Between 1985 and 1989, Shell, Amoco and Exxon drilled 12 exploratory wells from five locations and carried out one production test.

RESERVES

Five potentially commercial pay sands were logged between 5,500 and 13,500ft subsea. Estimated gross recovery from the planned development is about 250 million barrels of oil equivalent, with a 50:50 oil/gas ratio. The API gravity is 33°.

RAM POWELL TLP

Completely assembled, the Ram Powell TLP is 3,570ft high, from the seafloor to the crown block of the drilling rig. It was designed and engineered by a joint partner team made up of personnel from Shell, Amoco and Exxon, with support from outside contractors in Louisiana and Texas. It was designed to simultaneously withstand hurricane-force waves.

HULL

The contract for the hull fabrication was won by Belleli SpA in Taranto, Italy. It was completed in October 1996 and the structure arrived at Aker Gulf Marine's Ingleside yard, in Texas, in November 1996.

The hull is comprised of four circular steel columns, 66.5ft in diameter and 165ft-high. These are connected by a ring pontoon structure, 27ft wide and 24.5ft high, with a rectangular cross section. The hull weighs approximately 15,000t.

DECK

The contract for the modular deck was won by McDermott International and it was built at Morgan City, Louisiana. The first module was loaded out on 6 November 1996 with shipment of the remaining modules concluded by the end of December 1996.

The deck is an open truss/deep girder design. It measures 245ftx245ft and stands 40ft high. The structure weighs approximately 8,100t and is composed of five modules, namely: wellbay, quarters, process, power and drilling. The accommodation module houses up to 110 people, along with a control room and an emergency-response centre.

TENDONS/PILES

The TLP is secured by 12 tendons, three per corner, each with a diameter of 28in and a wall thickness of 1.2in. Each tendon is approximately 3,145ft long and the total weight for the 12 tendons is approximately 10,000t. The tendons will be attached by the TLP foundation system, comprising tendon receptacles held in place by 12 piles. The piles are 84in in diameter and 349ft long, weighing approximately 270t each. Aker Gulf Marine fabricated the tendons and piles in Corpus Christi, Texas.

DRILLING

The well layout on the seafloor is arranged in a rectangular pattern approximately 60ftx80ft. The drilling programme envisaged pre-drilling four development wells from the 20-slot template. The TLP supports a single modified API Helmlich & Payne



Expand Image

The Ram Powell tension leg platform (TLP) is located in 3,214ft of water at Viosca Knoll, block 956, in the Gulf Of Mexico.



Expand Image

The Sea-Aker Star tows the Ram Powell TLP to site. The TLP is 3,570ft high, from the seafloor to the crown block of the drilling rig.



Expand Image

The Sea-Aker Star, with the Ram Powell TLP in the background.



Expand Image

The Mighty Servant 2, with the Belleli-built Ram Powell hull loaded.

platform-type drilling rig (leased), equipped with a surface BOP and a high-pressure drilling riser.

PRODUCTION

The Ram Powell TLP contains complete separation, dehydration and treatment facilities designed to process the oil, condensate and gas. Estimated ultimate recovery from the development is about 250 million barrels of oil equivalent.

EXPORT

Ram Powell's oil and gas is piped to platforms in shallow water. Production from the platform is transported approximately 25 miles via a 12in-diameter oil pipeline to Main Pass 289C and a 14in gas pipeline to Viosca Knoll 817. Both pipelines are installed as part of the Ram-Powell development.

Allseas laid the pipelines using the Lorelay.



[Expand Image](#)
Towing of the TLP, out into the Gulf Of Mexico.



[Expand Image](#)
Platform integration, taking place at the Aker-Gulf marine yard, in Ingleside, Texas.

Post to:

[Delicious](#) [Digg](#) [reddit](#) [Facebook](#) [StumbleUpon](#)

APPENDIX III: Surge Calculation (Microsoft Excel)

ω_0 0.368918
 f_0 0.058715
 L
 stiffness k 240103
 mass surge 64061100
 c 156875.8
 current 0 m/s

t	$s(f)$	$h(f)$	r.number	at t=0 total force	Absolute total force	ϵ	$\omega=2\pi f$	$F_i/(H/2)$	$(k-m\omega^2)$	$(k-m\omega^2)^2$	$(C\omega)^2$	rao	rao2 s(f)	surge h(f)
0.005	0	0	0.123057	0	0	0.773288	0.031416	0	176877.23	31285553980	24289116	0	0	0
0.015	2.3516E-122	4.34E-62	0.804881	-1.57883E-56	1.57883E-56	5.056616	0.094248	728010.9	-328928.9	1.08194E+11	218602043	2.211045	1.1496E-121	9.59E-62
0.025	1.55571E-12	3.53E-07	0.821719	-0.239354743	0.239354743	5.163679	0.15708	1356948	-1340541	1.79705E+12	607227896	1.012068	1.59348E-12	3.57E-07
0.035	0.477382849	0.195424	0.408612	149055.9239	149055.9239	2.56772	0.219911	1525460	-2857960	8.16793E+12	1.19E+09	0.53372	0.135985617	0.104302
0.045	72.32158079	2.405354	0.838959	-4511509.484	4511509.484	5.27202	0.282743	3751223	-4881184	2.3826E+13	1.967E+09	0.768475	42.70979125	1.848454
0.055	195.8156303	3.957935	0.394628	7484287.497	7484287.497	2.47984	0.345575	3781915	-7410215	5.49113E+13	2.939E+09	0.510351	51.00186133	2.019938
0.065	187.3866196	3.871812	0.291153	15364306.12	15364306.12	1.829603	0.408407	7936494	-10445052	1.09099E+14	4.105E+09	0.759819	108.1828264	2.941875
0.075	131.6824579	3.245704	0.373205	11669073.64	11669073.64	2.345218	0.471239	7190472	-13985696	1.956E+14	5.465E+09	0.514123	34.80667112	1.668692
0.085	84.7333993	2.603588	0.187640	14495158.28	14495158.28	1.17913	0.534071	11134755	-18032145	3.25158E+14	7.02E+09	0.617488	32.30812641	1.607685
0.095	53.81677326	2.074932	0.654361	-11801758.38	11801758.38	4.112007	0.596903	11375563	-22584400	5.10055E+14	8.768E+09	0.503687	13.65333805	1.045116
0.105	34.65150158	1.664969	0.291859	12264163.74	12264163.74	1.834042	0.659734	14732007	-27642462	7.64106E+14	1.071E+10	0.532945	9.842067683	0.887336
0.115	22.82288797	1.351233	0.070757	4861995.406	4861995.406	0.444635	0.722566	7196383	-33206330	1.10266E+15	1.285E+10	0.216716	1.071895062	0.292834
0.125	15.40890805	1.110276	0.257203	9791030.833	9791030.833	1.616264	0.785398	17637113	-39276004	1.5426E+15	1.518E+10	0.449053	3.107191157	0.498573
0.135	10.65750529	0.923364	0.123726	6013912.408	6013912.408	0.777494	0.84823	13026097	-45851484	2.10236E+15	1.771E+10	0.284092	0.860149108	0.26232
0.145	7.538999201	0.776608	0.956782	-1975939.384	1975939.384	6.012418	0.911062	5088641	-52932771	2.80188E+15	2.043E+10	0.096134	0.069673049	0.074658
0.155	5.443932632	0.659935	0.091329	3541118.175	3541118.175	0.573914	0.973894	10731713	-60519863	3.66265E+15	2.334E+10	0.177325	0.171179676	0.117023
0.165	4.005205516	0.566053	0.054246	1909353.389	1909353.389	0.340884	1.036726	6746195	-68612762	4.70771E+15	2.645E+10	0.098322	0.038719558	0.055656
0.175	2.996952172	0.489649	0.770812	-4936315.357	4936315.357	4.843784	1.099557	20162668	-77211467	5.96161E+15	2.975E+10	0.261135	0.204366648	0.127865
0.185	2.277102129	0.426812	0.678994	-3951287.263	3951287.263	4.266796	1.162389	18515368	-86315978	7.45045E+15	3.325E+10	0.214506	0.104776258	0.091554
0.195	1.754340928	0.37463	0.433329	1566381.775	1566381.775	2.723041	1.225221	8362298	-95926295	9.20185E+15	3.694E+10	0.087174	0.013331781	0.032658
0.205	1.368758319	0.330909	0.571320	-1487829.896	1487829.896	3.590174	1.288053	8992385	-1.06E+08	1.1245E+16	4.083E+10	0.0848	0.009842734	0.028061
0.215	1.080282859	0.293977	0.976742	-438552.2281	438552.2281	6.137844	1.350885	2983579	-1.17E+08	1.36106E+16	4.491E+10	0.025574	0.000706537	0.007518
0.225	0.861626927	0.262546	0.398169	1624144.864	1624144.864	2.502095	1.413717	12372291	-1.28E+08	1.63308E+16	4.919E+10	0.096816	0.00807626	0.025419
0.235	0.693896127	0.235609	0.608733	-1545560.747	1545560.747	3.825281	1.476549	13119698	-1.39E+08	1.94395E+16	5.365E+10	0.094098	0.006144064	0.02217
0.245	0.563804025	0.212378	0.029737	410853.3132	410853.3132	0.186868	1.53938	3869080	-1.52E+08	2.29719E+16	5.832E+10	0.025528	0.000367405	0.005421
0.255	0.461872914	0.192223	0.920205	-956100.6297	956100.6297	5.782566	1.602212	9947807	-1.64E+08	2.6965E+16	6.318E+10	0.06058	0.001695026	0.011645

838.8214206

Mo

8.388214

Diameter	20.24 m
Draft	25 m
d	980 m
T (Period)	66.66666667 sec
H	4.33739E-62 m
Cm	1.6
Cd	0.65
p	1030 kg/m³
g	9.806 m/sec²
x	0
t	0
current	0
ε	5.056615777
pontoon	
height	7.47
pontoon	
length	54.41
pontoon	
diameter	8.846819

Δ	1 m
g	9
f	0.015
	0.001
L	6935.426834
k	0.000906073
w	0.09426
Centre of gravity	3 m

Total Force -1.57883E-56

h	s	u	u'	force
980	979.5	9.70798E-64	-2.55E-64	-1.3536E-58
979	978.5	9.70174E-64	-2.55E-64	-1.35273E-58
978	977.5	9.6955E-64	-2.55E-64	-1.35187E-58
977	976.5	9.68928E-64	-2.55E-64	-1.351E-58
976	975.5	9.68306E-64	-2.55E-64	-1.35013E-58
975	974.5	9.67685E-64	-2.54E-64	-1.34926E-58
974	973.5	9.67064E-64	-2.54E-64	-1.3484E-58
973	972.5	9.66445E-64	-2.54E-64	-1.34754E-58
972	971.5	9.65826E-64	-2.54E-64	-1.34667E-58
971	970.5	9.65208E-64	-2.54E-64	-1.34581E-58
970	969.5	9.64591E-64	-2.54E-64	-1.34495E-58
969	968.5	9.63975E-64	-2.53E-64	-1.34409E-58
968	967.5	9.63359E-64	-2.53E-64	-1.34323E-58
967	966.5	9.62745E-64	-2.53E-64	-1.34238E-58
966	965.5	9.62131E-64	-2.53E-64	-1.34152E-58
965	964.5	9.61518E-64	-2.53E-64	-1.34066E-58
964	963.5	9.60905E-64	-2.53E-64	-1.33981E-58
963	962.5	9.60294E-64	-2.52E-64	-1.33896E-58
962	961.5	9.59683E-64	-2.52E-64	-1.33811E-58
961	960.5	9.59073E-64	-2.52E-64	-1.33726E-58
960	959.5	9.58464E-64	-2.52E-64	-1.33641E-58
959	958.5	9.57855E-64	-2.52E-64	-1.33556E-58
958	957.5	9.57247E-64	-2.52E-64	-1.33471E-58
957	956.5	9.56641E-64	-2.52E-64	-1.33386E-58
956	955.5	9.56035E-64	-2.51E-64	-1.33302E-58
				-3.35815E-57

pontoon

h	s	u	u'	Force
950	951.5	9.77214E-64	-2.51E-64	-1.67946E-58
951	952.5	9.77832E-64	-2.51E-64	-1.68052E-58
952	953.5	9.78451E-64	-2.51E-64	-1.68159E-58
953	954.5	9.7907E-64	-2.51E-64	-1.68265E-58
954	955.5	9.79691E-64	-2.51E-64	-1.68372E-58
955	956.5	9.80312E-64	-2.52E-64	-1.68478E-58
956	957.5	9.80934E-64	-2.52E-64	-1.68585E-58
				-1.17786E-57

APPENDIX IV: Heave Calculation (Microsoft Excel)

$$P = \rho g \frac{H \cosh ks}{2 \cosh kd} \cos \Theta$$

(Dynamic Pressure)

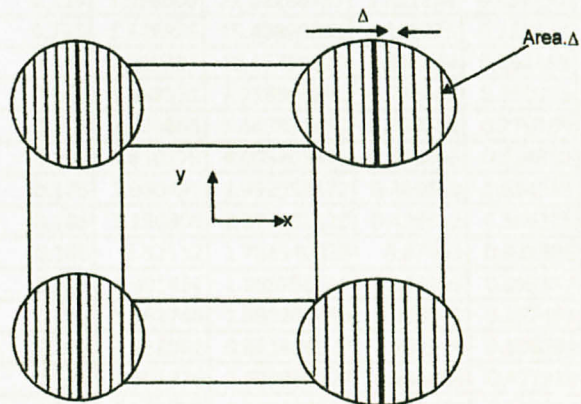
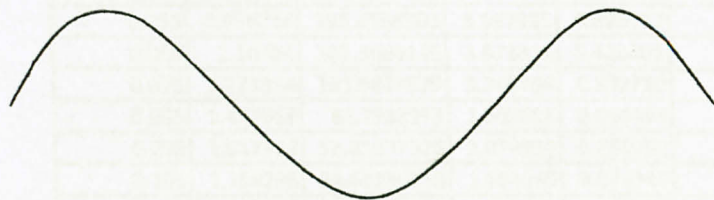
$$P = \rho g d_{draft}$$

(Hydronic Pressure)

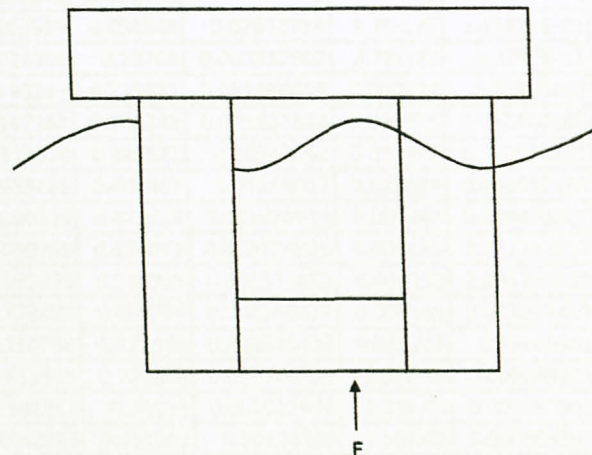
$$P = \rho g \left(d_{draft} + \frac{H \cosh ks}{2 \cosh kd} \cos \Theta \right)$$

$$F = P \cdot A$$

(Force)



(Total Pressure)



d	980.2 m	k	0.00090598
D	20.25 m	ω	0.09426
draft	25 m	T	66.66666667
ρ (density)	1030	L	6936.134097
g (gravity)	9.807		
H	4.33739E-62 m		
t	0 sec		
f	0.015 Hz		
r	10.125 m		
s	955.2 m		
ε	6.116247898		

ω_0 0.36891804
 f_0 0.05871513

L
 stiffness k 1213040285
 mass heave 73273230.1
 c 11925326.3

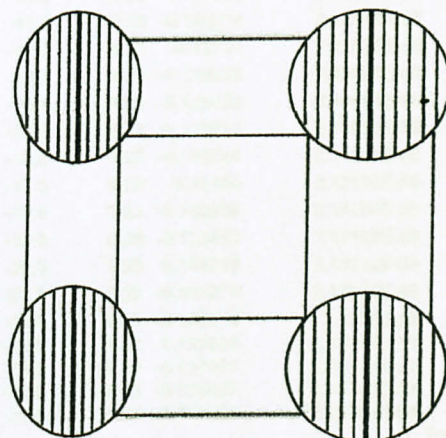
f	f/f ₀	S(f)	h(f)	r.number	Total Pressure	ε	$\omega=2\pi f$	rao	rao2 s(f)	heave h(f)
0.005	0.085157	0	0	0.973305	0	6.116248	0.031416	0	0	0
0.015	0.255471	2.3516E-122	4.34E-62	0.662564	7.02737E-55	4.163553	0.094248	0.02672714	1.7E-125	1.15926E-63
0.025	0.425785	1.55571E-12	3.53E-07	0.751330	0.050742795	4.721356	0.15708	0.000237502	8.78E-20	8.3787E-11
0.035	0.596098	0.477382849	0.195424	0.078353	2560550.768	0.49237	0.219911	0.021666043	0.000224	0.00423407
0.045	0.766412	72.32158079	2.405354	0.500822	31652812.14	3.147162	0.282743	0.021801644	0.034375	0.052440666
0.055	0.936726	195.8156303	3.957935	0.696797	18638332.22	4.378674	0.345575	0.00782052	0.011976	0.030953111
0.065	1.10704	187.3866196	3.871812	0.420001	29199368.7	2.639285	0.408407	0.01256057	0.029564	0.048632168
0.075	1.277354	131.6824579	3.245704	0.302720	3243487.304	1.90229	0.471239	0.001670013	0.000367	0.005420367
0.085	1.447668	84.7333993	2.603588	0.014443	12655770.88	0.090759	0.534071	0.008154825	0.005635	0.021231807
0.095	1.617982	53.81677326	2.074932	0.268952	1935607.953	1.690093	0.596903	0.001571853	0.000133	0.003261487
0.105	1.788295	34.65150158	1.664969	0.075349	1935607.953	0.473491	0.659734	0.001968477	0.000134	0.003277453
0.115	1.958609	22.82288797	1.351233	0.437737	20494141.91	2.750738	0.722566	0.025820422	0.015216	0.03488941
0.125	2.128923	15.40890805	1.110276	0.129458	495876.8445	0.813515	0.785398	0.000764855	9.01E-06	0.000849201
0.135	2.299237	10.65750529	0.923364	0.567369	1083734.673	3.565347	0.84823	0.002022976	4.36E-05	0.001867943
0.145	2.469551	7.538999201	0.776608	0.150053	555962.2324	0.942935	0.911062	0.00124258	1.16E-05	0.000964997
0.155	2.639865	5.443932632	0.659935	0.279789	33725.24926	1.758192	0.973894	8.93749E-05	4.35E-08	5.89817E-05
0.165	2.810179	4.005205516	0.566053	0.394322	139341.8056	2.477916	1.036726	0.000434024	7.54E-07	0.000245681
0.175	2.980492	2.996952172	0.489649	0.684283	70066.96614	4.300034	1.099557	0.000254506	1.94E-07	0.000124618
0.185	3.150806	2.277102129	0.426812	0.566325	32697.6523	3.558789	1.162389	0.000137527	4.31E-08	5.8698E-05
0.195	3.32112	1.754340928	0.37463	0.921886	63041.8863	5.793129	1.225221	0.000305096	1.63E-07	0.000114298
0.205	3.491434	1.368758319	0.330909	0.099157	45655.90473	0.177006	1.288053	0.000252799	8.75E-08	8.36533E-05
0.215	3.661748	1.080282859	0.293977	0.257461	14561.76831	0.97834	1.350885	9.17791E-05	9.1E-09	2.6981E-05
0.225	3.832062	0.861626927	0.262546	0.306292	16532.22784	0.95146	1.413717	0.000118064	1.2E-08	3.09972E-05
0.235	4.002376	0.693896127	0.235609	0.477924	2563.775186	0.265653	1.476549	2.06598E-05	2.96E-10	4.86764E-06
0.245	4.172689	0.563804025	0.212378	0.113004	3259.691415	0.236775	1.53938	2.953E-05	4.92E-10	6.27152E-06
0.255	4.343003	0.461872914	0.192223	0.406328	63041.8863	0.351327	1.602212	0.000639881	1.89E-07	0.000123

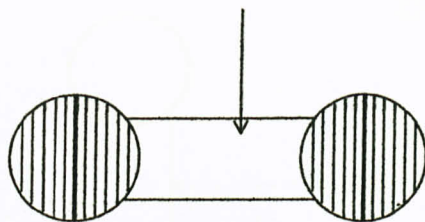
833.7911794

Mo 8.337912
 Hs 11.55018

For column

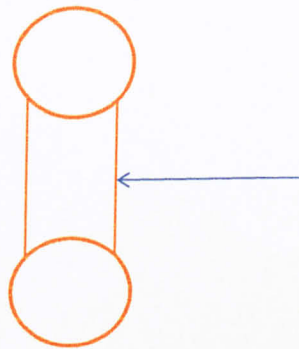
x	x(point)	Total	Θ	Dynamic Pressure	Total Pressure	Force P.A
47	47.05	0.355424289	-6.073622	2.10878E-58	2.10878E-58	7.49513E-59
46	46.5	6.381724289	-6.07412	2.10901E-58	2.10901E-58	1.34591E-57
45	45.5	11.00172429	-6.075026	2.10941E-58	2.10941E-58	2.32072E-57
44	44.5	13.67862429	-6.075932	2.10982E-58	2.10982E-58	2.88594E-57
43	43.5	14.78802429	-6.076838	2.11022E-58	2.11022E-58	3.12059E-57
42	42.5	17.11712429	-6.077744	2.11062E-58	2.11062E-58	3.61277E-57
41	41.5	18.26282429	-6.07865	2.11101E-58	2.11101E-58	3.85531E-57
40	40.5	19.12882429	-6.079556	2.11141E-58	2.11141E-58	4.03888E-57
39	39.5	19.75302429	-6.080462	2.1118E-58	2.1118E-58	4.17145E-57
38	38.5	20.15812429	-6.081368	2.1122E-58	2.1122E-58	4.25779E-57
37	37.5	20.40572429	-6.082274	2.11259E-58	2.11259E-58	4.31089E-57
36	36.5	20.40572429	-6.08318	2.11298E-58	2.11298E-58	4.31168E-57
35	35.5	20.15812429	-6.084086	2.11336E-58	2.11336E-58	4.26014E-57
34	34.5	19.75302429	-6.084992	2.11375E-58	2.11375E-58	4.17529E-57
33	33.5	19.12882429	-6.085898	2.11413E-58	2.11413E-58	4.04409E-57
32	32.5	18.26282429	-6.086804	2.11451E-58	2.11451E-58	3.8617E-57
31	31.5	17.11712429	-6.08771	2.11489E-58	2.11489E-58	3.62009E-57
30	30.5	14.78802429	-6.088616	2.11527E-58	2.11527E-58	3.12807E-57
29	29.5	13.67862429	-6.089521	2.11565E-58	2.11565E-58	2.89392E-57
28	28.5	11.00172429	-6.090427	2.11602E-58	2.11602E-58	2.32799E-57
27	27.5	6.381724289	-6.091333	2.1164E-58	2.1164E-58	1.35063E-57
26	26.5	0.355424289	-6.092239	2.11677E-58	2.11677E-58	7.52351E-59
-26	-26.5	0.355424289	-6.140256	2.13397E-58	2.13397E-58	7.58464E-59
-27	-27.5	6.381724289	-6.141162	2.13425E-58	2.13425E-58	1.36202E-57
-28	-28.5	11.00172429	-6.142068	2.13452E-58	2.13452E-58	2.34834E-57
-29	-29.5	13.67862429	-6.142974	2.1348E-58	2.1348E-58	2.92011E-57
-30	-30.5	14.78802429	-6.14388	2.13507E-58	2.13507E-58	3.15734E-57
-31	-31.5	17.11712429	-6.144786	2.13534E-58	2.13534E-58	3.65509E-57
-32	-32.5	18.26282429	-6.145692	2.13561E-58	2.13561E-58	3.90022E-57
-33	-33.5	19.12882429	-6.146598	2.13587E-58	2.13587E-58	4.08568E-57
-34	-34.5	19.75302429	-6.147504	2.13614E-58	2.13614E-58	4.21952E-57
-35	-35.5	20.15812429	-6.14841	2.1364E-58	2.1364E-58	4.30659E-57
-36	-36.5	20.40572429	-6.149316	2.13666E-58	2.13666E-58	4.36002E-57
-37	-37.5	20.40572429	-6.150222	2.13692E-58	2.13692E-58	4.36055E-57
-38	-38.5	20.15812429	-6.151128	2.13718E-58	2.13718E-58	4.30816E-57
-39	-39.5	19.75302429	-6.152034	2.13744E-58	2.13744E-58	4.22209E-57
-40	-40.5	19.12882429	-6.15294	2.13769E-58	2.13769E-58	4.08915E-57
-41	-41.5	18.26282429	-6.153846	2.13795E-58	2.13795E-58	3.90449E-57
-42	-42.5	17.11712429	-6.154752	2.1382E-58	2.1382E-58	3.65998E-57
-43	-43.5	14.78802429	-6.155658	2.13845E-58	2.13845E-58	3.16234E-57
-44	-44.5	13.67862429	-6.156564	2.13869E-58	2.13869E-58	2.92544E-57
-45	-45.5	11.00172429	-6.15747	2.13894E-58	2.13894E-58	2.3532E-57
-46	-46.5	6.381724289	-6.158376	2.13918E-58	2.13918E-58	1.36517E-57
-47	-47.5	0.355424289	-6.159282	2.13943E-58	2.13943E-58	7.60404E-59
		644.1246687			Total Force	6.8044E-56





For pontoon

x	x(point)	Total	Θ	Dynamic Pressure	Total Pressure	Force P.A
26	26.5	8.23	-6.092692	2.11695E-58	2.11695E-58	1.74225E-57
25	25.5	8.23	-6.093598	2.11732E-58	2.11732E-58	1.74256E-57
24	24.5	8.23	-6.094504	2.11769E-58	2.11769E-58	1.74286E-57
23	23.5	8.23	-6.09541	2.11806E-58	2.11806E-58	1.74316E-57
22	22.5	8.23	-6.096316	2.11842E-58	2.11842E-58	1.74346E-57
21	21.5	8.23	-6.097222	2.11878E-58	2.11878E-58	1.74376E-57
20	20.5	8.23	-6.098128	2.11914E-58	2.11914E-58	1.74405E-57
19	19.5	8.23	-6.099034	2.1195E-58	2.1195E-58	1.74435E-57
18	18.5	8.23	-6.09994	2.11986E-58	2.11986E-58	1.74464E-57
17	17.5	8.23	-6.100846	2.12021E-58	2.12021E-58	1.74493E-57
16	16.5	8.23	-6.101752	2.12057E-58	2.12057E-58	1.74523E-57
15	15.5	8.23	-6.102658	2.12092E-58	2.12092E-58	1.74551E-57
14	14.5	8.23	-6.103564	2.12127E-58	2.12127E-58	1.7458E-57
13	13.5	8.23	-6.10447	2.12162E-58	2.12162E-58	1.74609E-57
12	12.5	8.23	-6.105376	2.12196E-58	2.12196E-58	1.74637E-57
11	11.5	8.23	-6.106282	2.12231E-58	2.12231E-58	1.74666E-57
10	10.5	8.23	-6.107188	2.12265E-58	2.12265E-58	1.74694E-57
9	9.5	8.23	-6.108094	2.12299E-58	2.12299E-58	1.74722E-57
8	8.5	8.23	-6.109	2.12333E-58	2.12333E-58	1.7475E-57
7	7.5	8.23	-6.109906	2.12367E-58	2.12367E-58	1.74778E-57
6	6.5	8.23	-6.110812	2.124E-58	2.124E-58	1.74805E-57
5	5.5	8.23	-6.111718	2.12434E-58	2.12434E-58	1.74833E-57
4	4.5	8.23	-6.112624	2.12467E-58	2.12467E-58	1.7486E-57
3	3.5	8.23	-6.11353	2.125E-58	2.125E-58	1.74888E-57
2	2.5	8.23	-6.114436	2.12533E-58	2.12533E-58	1.74915E-57
1	1.5	8.23	-6.115342	2.12566E-58	2.12566E-58	1.74942E-57
0	0.5	8.23	-6.116248	2.12598E-58	2.12598E-58	1.74968E-57
0	-0.5	8.23	-6.116248	2.12598E-58	2.12598E-58	1.74968E-57
-1	-1.5	8.23	-6.117154	2.12631E-58	2.12631E-58	1.74995E-57
-2	-2.5	8.23	-6.11806	2.12663E-58	2.12663E-58	1.75021E-57
-3	-3.5	8.23	-6.118966	2.12695E-58	2.12695E-58	1.75048E-57
-4	-4.5	8.23	-6.119872	2.12727E-58	2.12727E-58	1.75074E-57
-5	-5.5	8.23	-6.120778	2.12758E-58	2.12758E-58	1.751E-57
-6	-6.5	8.23	-6.121684	2.1279E-58	2.1279E-58	1.75126E-57
-7	-7.5	8.23	-6.12259	2.12821E-58	2.12821E-58	1.75152E-57
-8	-8.5	8.23	-6.123496	2.12852E-58	2.12852E-58	1.75177E-57
-9	-9.5	8.23	-6.124402	2.12883E-58	2.12883E-58	1.75203E-57
-10	-10.5	8.23	-6.125308	2.12914E-58	2.12914E-58	1.75228E-57
-11	-11.5	8.23	-6.126214	2.12945E-58	2.12945E-58	1.75253E-57
-12	-12.5	8.23	-6.12712	2.12975E-58	2.12975E-58	1.75278E-57
-13	-13.5	8.23	-6.128026	2.13005E-58	2.13005E-58	1.75303E-57
-14	-14.5	8.23	-6.128932	2.13035E-58	2.13035E-58	1.75328E-57
-15	-15.5	8.23	-6.129838	2.13065E-58	2.13065E-58	1.75353E-57
-16	-16.5	8.23	-6.130744	2.13095E-58	2.13095E-58	1.75377E-57
-17	-17.5	8.23	-6.13165	2.13125E-58	2.13125E-58	1.75402E-57
-18	-18.5	8.23	-6.132556	2.13154E-58	2.13154E-58	1.75426E-57
-19	-19.5	8.23	-6.133462	2.13183E-58	2.13183E-58	1.7545E-57
-20	-20.5	8.23	-6.134368	2.13212E-58	2.13212E-58	1.75474E-57
-21	-21.5	8.23	-6.135273	2.13241E-58	2.13241E-58	1.75498E-57
-22	-22.5	8.23	-6.136179	2.1327E-58	2.1327E-58	1.75521E-57
-23	-23.5	8.23	-6.137085	2.13298E-58	2.13298E-58	1.75545E-57
-24	-24.5	8.23	-6.137991	2.13327E-58	2.13327E-58	1.75568E-57
-25	-25.5	8.23	-6.138897	2.13355E-58	2.13355E-58	1.75591E-57
-26	-26.5	8.23	-6.139803	2.13383E-58	2.13383E-58	1.75614E-57
Total force						9.4474E-56



x	x(point)	Total Area	Θ	Dynamic Pressure	Total Pressure	Force P.A
40	40.5	55.55	-6.079556	2.11141E-58	2.11141E-58	1.17289E-56
39	39.5	55.55	-6.080462	2.1118E-58	2.1118E-58	1.17311E-56
38	38.5	55.55	-6.081368	2.1122E-58	2.1122E-58	1.17332E-56
37	37.5	55.55	-6.082274	2.11259E-58	2.11259E-58	1.17354E-56
36	36.5	55.55	-6.08318	2.11298E-58	2.11298E-58	1.17376E-56
35	35.5	55.55	-6.084086	2.11336E-58	2.11336E-58	1.17397E-56
34	34.5	55.55	-6.084992	2.11375E-58	2.11375E-58	1.17419E-56
33	33.5	55.55	-6.085898	2.11413E-58	2.11413E-58	1.1744E-56
-33	-33.5	55.55	-6.146598	2.13587E-58	2.13587E-58	1.18648E-56
-34	-34.5	55.55	-6.147504	2.13614E-58	2.13614E-58	1.18663E-56
-35	-35.5	55.55	-6.14841	2.1364E-58	2.1364E-58	1.18677E-56
-36	-36.5	55.55	-6.149316	2.13666E-58	2.13666E-58	1.18692E-56
-37	-37.5	55.55	-6.150222	2.13692E-58	2.13692E-58	1.18706E-56
-38	-38.5	55.55	-6.151128	2.13718E-58	2.13718E-58	1.1872E-56
-39	-39.5	55.55	-6.152034	2.13744E-58	2.13744E-58	1.18735E-56
-40	-40.5	55.55	-6.15294	2.13769E-58	2.13769E-58	1.18749E-56
total force						1.88851E-55

APPENDIX V: Pitch Calculation (Microsoft Excel)

ω_0 0.368918036
 f_0 0.058715129
 L
 c 25294744714
moment inertia 251578858149
 k pitch 1589521757809

f	f/t ₀					S(f)	h(f)	r.number	Total moment	Absolute Moment	ε	ω=2πf	RAO	RAO ² S(f)	Pitch h(f)
0.005	0.085156928	19016.04	0.0000000	0.778877	1558.545	0	0	0.4950242	0	0	3.110732	0.031416	0	0	0
0.015	0.255470783	234.7659	0.0000000	0.778877	1558.545	2.3516E-122	4.33739E-62	0.5985485	-6.73244E-56	6.73244E-56	3.761279	0.094248	1.95577E-06	8.9951E-134	8.48295E-68
0.025	0.425784639	30.42566	0.0000000	0.778877	1558.545	1.55571E-12	3.52784E-07	0.0731963	0.807375243	0.807375243	0.459966	0.15708	2.89087E-06	1.30012E-23	1.01985E-12
0.035	0.596098494	7.92005	0.0000502	0.778877	1558.545	0.477382849	0.195424226	0.0094355	112446.5441	112446.5441	0.059292	0.219911	7.29569E-07	2.54097E-13	1.42575E-07
0.045	0.76641235	2.898345	0.0267043	0.778877	1558.545	72.32158079	2.405353709	0.1992595	33613954.42	33613954.42	1.252147	0.282743	1.78087E-05	2.29367E-08	4.28361E-05
0.055	0.936726205	1.298821	0.1972021	0.778877	1558.545	195.8156303	3.957935121	0.7431892	-80083313.96	80083313.96	4.670201	0.345575	2.59489E-05	1.31852E-07	0.000102704
0.065	1.107040061	0.665804	0.4350669	0.778877	1558.545	187.3866196	3.871812181	0.4003821	56724625.87	56724625.87	2.516001	0.408407	1.89336E-05	6.71747E-08	7.33074E-05
0.075	1.277353916	0.375625	0.6252949	0.778877	1558.545	131.6824579	3.245704335	0.4935164	2268557.933	2268557.933	3.101257	0.471239	9.11453E-07	1.09395E-10	2.95831E-06
0.085	1.447667772	0.22768	0.7523154	0.778877	1558.545	84.7333993	2.603588282	0.2692081	89548004.03	89548004.03	1.691704	0.534071	4.53208E-05	1.7404E-07	0.000117997
0.095	1.617981627	0.145917	0.8332712	0.778877	1558.545	53.81677326	2.074931773	0.1654503	67455007.97	67455007.97	1.03969	0.596903	4.33478E-05	1.01123E-07	8.99437E-05
0.105	1.788295483	0.097778	0.8849510	0.778877	1558.545	34.65150158	1.664968506	0.0868928	34314328.66	34314328.66	0.546035	0.659734	2.78492E-05	2.68748E-08	4.6368E-05
0.115	1.958609338	0.067953	0.9185662	0.778877	1558.545	22.82288797	1.351233154	0.1912221	50276935.13	50276935.13	1.20164	0.722566	5.10312E-05	5.9435E-08	6.89551E-05
0.125	2.128923194	0.048681	0.9409631	0.778877	1558.545	15.40890805	1.110275931	0.2215114	42903522.74	42903522.74	1.391978	0.785398	5.3878E-05	4.47297E-08	5.98195E-05
0.135	2.29923705	0.035782	0.9562580	0.778877	1558.545	10.65750529	0.923363646	0.3909455	21962557.45	21962557.45	2.456701	0.84823	3.3771E-05	1.21547E-08	3.11829E-05
0.145	2.469550905	0.026886	0.9669508	0.778877	1558.545	7.538999201	0.776607968	0.0822502	13582648.23	13582648.23	0.51686	0.911062	2.5332E-05	4.83784E-09	1.9673E-05
0.155	2.639864761	0.020591	0.9745899	0.778877	1558.545	5.443932632	0.659935308	0.3417894	17897041.25	17897041.25	2.147804	0.973894	4.01451E-05	8.77358E-09	2.64931E-05
0.165	2.810178616	0.016035	0.9801560	0.778877	1558.545	4.005205516	0.566053391	0.8683759	-12091574.28	12091574.28	5.456874	1.036726	3.23822E-05	4.19989E-09	1.83301E-05
0.175	2.980492472	0.012672	0.9842847	0.778877	1558.545	2.996952172	0.489649031	0.7365406	-12469107.08	12469107.08	4.628421	1.099557	3.9617E-05	4.70374E-09	1.93984E-05
0.185	3.150806327	0.010146	0.9873971	0.778877	1558.545	2.277102129	0.426811633	0.1087099	5931938.143	5931938.143	0.683133	1.162389	2.22397E-05	1.12627E-09	9.49217E-06
0.195	3.321120183	0.00822	0.9897778	0.778877	1558.545	1.754340928	0.374629516	0.2670026	6912001.048	6912001.048	1.677844	1.225221	3.04419E-05	1.62577E-09	1.14045E-05
0.205	3.491434038	0.00673	0.9916234	0.778877	1558.545	1.368758319	0.330908848	0.2526177	5048762.068	5048762.068	1.58745	1.288053	2.60257E-05	9.2711E-10	8.61213E-06
0.215	3.661747894	0.005562	0.9930714	0.778877	1558.545	1.080282859	0.293977259	0.1101625	2283690.459	2283690.459	0.692261	1.350885	1.37392E-05	2.03921E-10	4.03902E-06
0.225	3.832061749	0.004637	0.9942201	0.778877	1558.545	0.861626927	0.262545528	0.7041294	-2351026.7	2351026.7	4.424749	1.413717	1.64734E-05	2.33822E-10	4.32502E-06
0.235	4.002375605	0.003897	0.9951406	0.778877	1558.545	0.693896127	0.235609189	0.4558243	437415.6738	437415.6738	2.8644	1.476549	3.56491E-06	8.81843E-12	8.39925E-07
0.245	4.17268946	0.003299	0.9958852	0.778877	1558.545	0.563804025	0.212377781	0.1931792	877763.2862	877763.2862	1.213938	1.53938	8.31624E-06	3.89926E-11	1.76618E-06
0.255	4.343003316	0.002811	0.9964926	0.778877	1558.545	0.461872914	0.192223394	0.3975531	267024.2393	267024.2393	2.498224	1.602212	2.94183E-06	3.99723E-12	5.65489E-07

838.8214206

Mo 8.388214206

HS 11.58496557

Diameter	20.24 m
Draft	25 m
d	960 m
T (Period)	66.66666667 sec
H	4.33739E-62 m
Cm	1.05
Cd	0.65
ρ	1030 kg/m ³
g	9.806 m/sec ²
x	0
l	0
current	0
s	3.761278705
pontoon	
height	7.47
pontoon	
length	54.41
pontoon	
diameter	8.846819

Δ	1 m
g	9
f	0.015
L	0.001
k	6935.427
w	0.000906
	0.09426
Centre of gravity	3 m

h	s	u	u'	Force	y	Moment
980	979.5	-2.34181E-63	-1.57483E-64	-5.48059E-59	3	1.64E-58
979	978.5	-2.34031E-63	-1.57382E-64	-5.47707E-59	2	1.1E-58
978	977.5	-2.3388E-63	-1.57281E-64	-5.47355E-59	1	5.47E-59
977	976.5	-2.3373E-63	-1.5718E-64	-5.47003E-59	0	0
976	975.5	-2.3358E-63	-1.57079E-64	-5.46652E-59	-1	-5.47E-59
975	974.5	-2.3343E-63	-1.56978E-64	-5.46302E-59	-2	-1.09E-58
974	973.5	-2.33281E-63	-1.56877E-64	-5.45952E-59	-3	-1.64E-58
973	972.5	-2.33131E-63	-1.56777E-64	-5.45602E-59	-4	-2.18E-58
972	971.5	-2.32982E-63	-1.56677E-64	-5.45253E-59	-5	-2.73E-58
971	970.5	-2.32833E-63	-1.56576E-64	-5.44904E-59	-6	-3.27E-58
970	969.5	-2.32684E-63	-1.56476E-64	-5.44555E-59	-7	-3.81E-58
969	968.5	-2.32535E-63	-1.56376E-64	-5.44207E-59	-8	-4.35E-58
968	967.5	-2.32387E-63	-1.56276E-64	-5.4386E-59	-9	-4.89E-58
967	966.5	-2.32238E-63	-1.56177E-64	-5.43513E-59	-10	-5.44E-58
966	965.5	-2.3209E-63	-1.56077E-64	-5.43166E-59	-11	-5.97E-58
965	964.5	-2.31942E-63	-1.55978E-64	-5.4282E-59	-12	-6.51E-58
964	963.5	-2.31795E-63	-1.55878E-64	-5.42474E-59	-13	-7.05E-58
963	962.5	-2.31647E-63	-1.55779E-64	-5.42129E-59	-14	-7.59E-58
962	961.5	-2.315E-63	-1.5568E-64	-5.41784E-59	-15	-8.13E-58
961	960.5	-2.31353E-63	-1.55581E-64	-5.4144E-59	-16	-8.66E-58
960	959.5	-2.31206E-63	-1.55482E-64	-5.41096E-59	-17	-9.2E-58
959	958.5	-2.31059E-63	-1.55383E-64	-5.40753E-59	-18	-9.73E-58
958	957.5	-2.30912E-63	-1.55285E-64	-5.40409E-59	-19	-1.03E-57
957	956.5	-2.30766E-63	-1.55186E-64	-5.40067E-59	-21	-1.13E-57
956	955.5	-2.3062E-63	-1.55088E-64	-5.39725E-59	-22	-1.19E-57
				-1.35968E-57	Total	-6.73E-56

pontoon

h	s	u	u'	Force	y	Moment
950	951.5	-2.2857E-63	-1.54696E-64	-6.79994E-59	-16	-1.08799E-57
951	952.5	-2.28714E-63	-1.54794E-64	-6.80424E-59	-17	-1.15672E-57
952	953.5	-2.28859E-63	-1.54892E-64	-6.80855E-59	-18	-1.22554E-57
953	954.5	-2.29004E-63	-1.5499E-64	-6.81286E-59	-19	-1.29444E-57
954	955.5	-2.29149E-63	-1.55088E-64	-6.81718E-59	-20	-1.36344E-57
955	956.5	-2.29294E-63	-1.55186E-64	-6.8215E-59	-21	-1.43251E-57
956	957.5	-2.2944E-63	-1.55285E-64	-6.82582E-59	-22	-1.50168E-57
				Total		-1.81247E-56